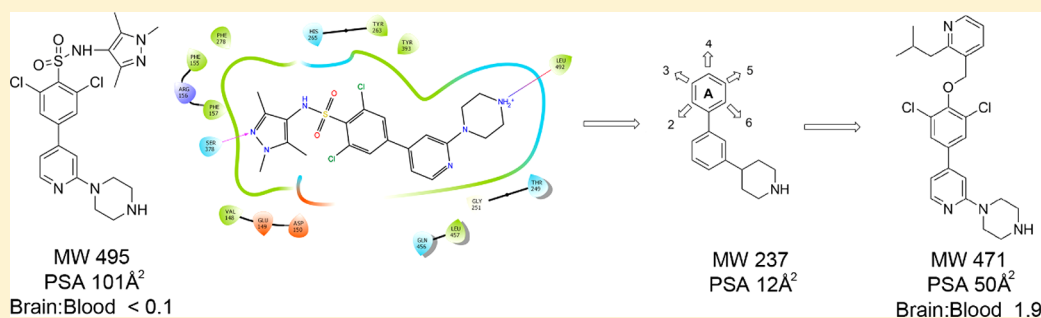


Design and Synthesis of Brain Penetrant Trypanocidal *N*-Myristoyltransferase Inhibitors

Tracy Bayliss, David A. Robinson,^{1b} Victoria C. Smith, Stephen Brand, Stuart P. McElroy, Leah S. Torrie, Chido Mpamhanga, Suzanne Norval, Laste Stojanovski, Ruth Brenk, Julie A. Frearson, Kevin D. Read, Ian H. Gilbert,^{1b} and Paul G. Wyatt*^{1b}

Drug Discovery Unit, College of Life Sciences, University of Dundee, Sir James Black Centre, Dundee DD1 5EH, U.K.

S Supporting Information



ABSTRACT: *N*-Myristoyltransferase (NMT) represents a promising drug target within the parasitic protozoa *Trypanosoma brucei* (*T. brucei*), the causative agent for human African trypanosomiasis (HAT) or sleeping sickness. We have previously validated *T. brucei* NMT as a promising druggable target for the treatment of HAT in both stages 1 and 2 of the disease. We report on the use of the previously reported DDD85646 (**1**) as a starting point for the design of a class of potent, brain penetrant inhibitors of *T. brucei* NMT.

INTRODUCTION

Human African trypanosomiasis (HAT) or sleeping sickness is prevalent in sub-Saharan Africa¹ with an estimated “at risk” population of 65 million.² The causative agents of HAT are the protozoan parasites *Trypanosoma brucei gambiense* and *Trypanosoma brucei rhodesiense*^{3,4} transmitted through the bite of an infected tsetse fly. HAT progresses through two stages. In the first stage (stage 1), the parasites proliferate solely within the bloodstream. In the second, late stage (stage 2), the parasite infects the central nervous system (CNS) causing the symptoms characteristic of the disease, such as disturbed sleep patterns and often death.⁵ Currently, there are a number of treatments available for HAT, though none are without issues, including toxicity and inappropriate routes of administration for a disease of rural Africa.⁶

Research has revealed enzymes and pathways that are crucial for the survival of *T. brucei*, and based on these studies, a number of antiparasitic drug targets have been proposed.^{7–10} *T. brucei* *N*-myristoyltransferase (*Tb*NMT) is one of the few *T. brucei* druggable targets to be genetically and chemically validated in both *in vitro* and in rodent models of HAT.^{7,11,12} NMT is a ubiquitous essential enzyme in all eukaryotic cells. It catalyzes the co- and post-translational transfer of myristic acid from myristoyl-CoA to the *N*-terminal glycine of a variety of peptides. Protein *N*-myristoylation facilitates membrane localization and biological activity of many important proteins.^{11,13}

NMT has been extensively investigated as a potential target for the treatment of other parasitic diseases including malaria,¹⁴ leishmaniasis,¹⁵ and Chagas’ disease^{16,17} resulting in the identification of multiple chemically distinct small molecule inhibitors.¹⁸ NMT has also been shown to be a potential therapeutic target for human diseases such as autoimmune disorders¹⁹ and cancer.^{20,21}

Previously we have reported the discovery of compound **1** (Figure 1),^{7,22,23} which showed excellent levels of inhibitory potency for *Tb*NMT and *T. brucei brucei* (*T. br. brucei*) proliferation *in vitro* and was used as a model compound to validate *Tb*NMT as a druggable target for stage 1 HAT.^{7,22} However, **1** is not blood–brain barrier penetrant, a requirement for stage 2 activity. Two approaches were taken to increase the brain penetration of **1**. A classical lead optimization approach is described elsewhere.²⁴ This article describes a second approach that used a minimum pharmacophore of **1** aiming to derive a structurally distinct series of potent *Tb*NMT inhibitors with brain penetration, as leads for the identification of suitable candidates for the treatment of stage 2 HAT.

COMPOUND RATIONALE AND DESIGN

To aid compound design, and to significantly lower molecular weight and polar surface area (PSA), the chlorines and the

Received: September 4, 2017

Published: November 10, 2017

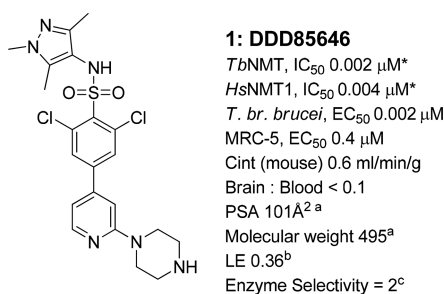


Figure 1. Compound 1. *Potencies were determined against recombinant *Tb*NMT and *Hs*NMT1, and against bloodstream form *T. brucei brucei* (*T. br. brucei*) and MRC-5 proliferation studies *in vitro* using 10 point curves replicated ≥ 2 . ^aCalculated using Optibrium STARDROP software. ^bLigand efficiency (LE), calculated as $0.6 \cdot \ln(\text{IC}_{50}) / (\text{heavy atom count})$ using *T. brucei* NMT IC₅₀ potency.²⁵ IC₅₀ values are shown as mean values of two or more determinations. Standard deviation was typically within 2-fold from the IC₅₀. ^cEnzyme selectivity calculated as *Hs*NMT1 IC₅₀ (μM)/*Tb*NMT IC₅₀ (μM).

sulfonamide moieties of **1** were removed to define a minimum pharmacophoric scaffold (Figure 2A). This scaffold was chosen because the piperidine makes a key interaction through the formation of a salt bridge with NMT's terminal carboxylate.¹⁰ This interaction is highly conserved across the binding modes of NMT inhibitors covering multiple chemotypes including **1** (Figure 2B); known antifungal NMT inhibitors such as Roche's (2-benzofurancarboxylic acid, 3-methyl-4-[3-[(3-pyridinylmethyl)amino]propoxy]-ethyl ester (RO-09-4609),^{26,27} Searle's *N*-[2-[4-[4-(2-methyl-1*H*-imidazol-1-yl)-

butyl]phenyl]acetyl]-L-seryl-*N*-(2-cyclohexylethyl)-L-lysineamide (SC-58272)²⁸ (Figure 2C), and Pfizer's 2-((1*R*,4*R*)-4-(aminomethyl)cyclohexanecarboxamido)-*N,N*-dimethylbenzo[*d*]thiazole-6-carboxamide (UK-370,485).²⁹ Attempts to crystallize *Tb*NMT had proved to be unsuccessful; therefore, the fungal *Aspergillus fumigatus* NMT (*Af*NMT)^{24,30} was used as a surrogate model for *Tb*NMT in this study. *Af*NMT is 42% identical to *Tb*NMT; however, within the peptide binding groove the level of identity is 92%. Previously, a selection of molecules from series **1** were assayed against *Af*NMT and *Tb*NMT using the SPA biochemical assay and pIC₅₀ values compared using linear regression analysis. The pIC₅₀ values were shown to be correlated with an *R*-squared value of 0.73 suggesting that *Af*NMT is a suitable surrogate system for study within this chemical series (see Supporting Information).

This minimum pharmacophoric scaffold had low molecular weight (237) and low PSA (12 Å² to maximize the potential for CNS penetration) from which we could design varied chemistry (Figure 2A) to either access the serine pocket (occupied by the pyrazole moiety in **1**) or the peptide recognition region, as seen in the peptomimetic compound highlighted in red (Figure 2C).

Compound Design. The adopted compound design strategy covered both compounds based on **1** (where common sulfonamide bioisosteres³¹ and pyrazole mimics were included) and compounds based on the binding pocket structural features, probing these with diverse hydrogen bond acceptor (HBA) and hydrogen bond donor (HBD) groups. We employed high throughput chemistry, using technologies and techniques such as scavengers and solid supported reagents enabling arrays to be made in parallel. Three different but complementary chemistries

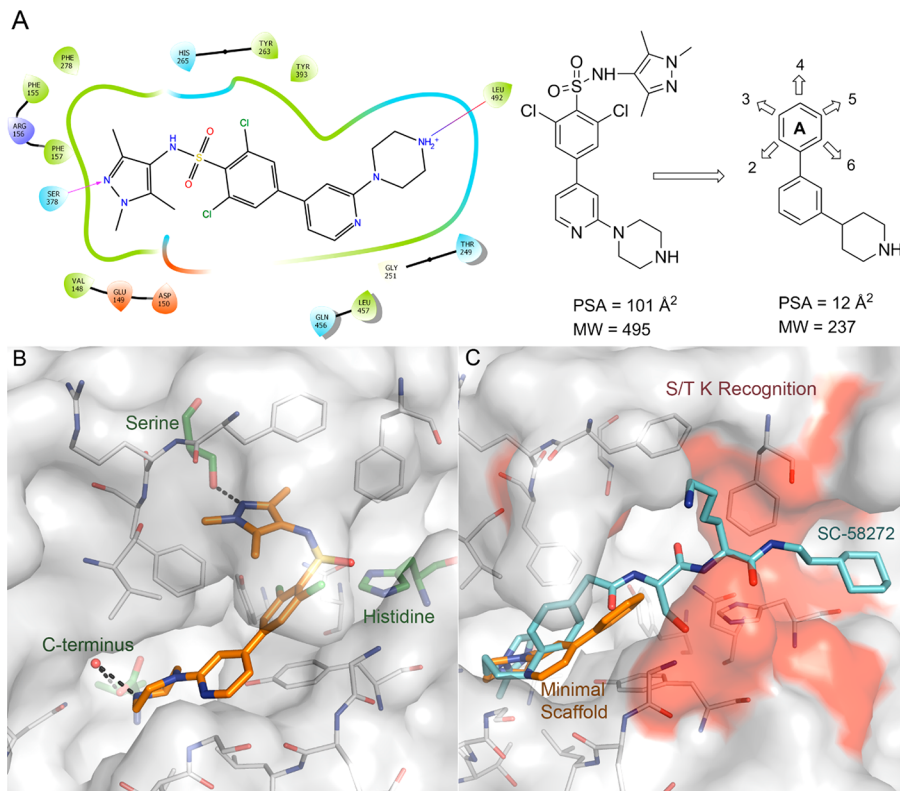


Figure 2. Development of the chemistry scaffold. (A) Two-dimensional interaction map of **1** bound to *Af*NMT leading to the design of the minimal scaffold. (B) Crystal structure of **1** bound; key recognition residues are highlighted and labeled. (C) Proposed minimal scaffold (C atoms gold) docked into the crystal structure of *Af*NMT overlaid with peptomimetic compound PDB 2NMT (C atoms cyan); the key S/T K peptide recognition region is highlighted red.

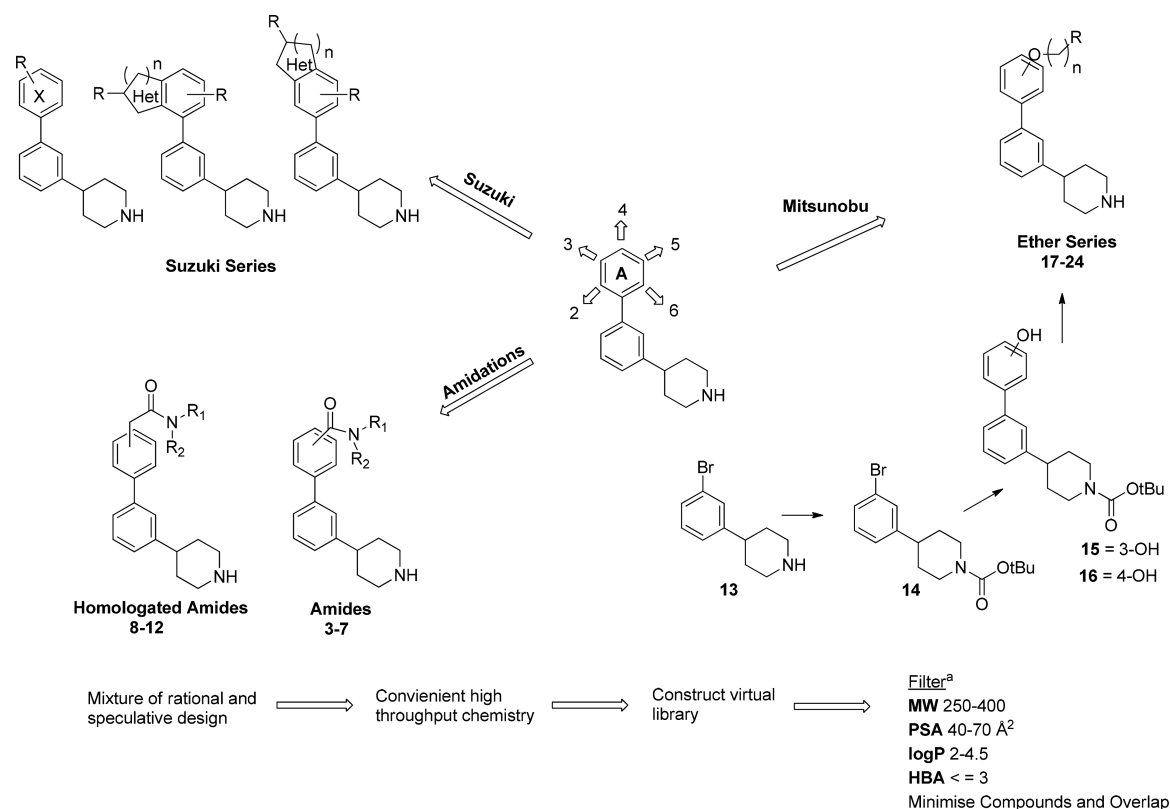


Figure 3. Scaffold array chemistry and design. ^aFilter parameters calculated using the Optibrium STARDROP software.

of Suzuki couplings, amidations, and Mitsunobu reactions were chosen to explore all positions around ring A (Figure 3).

Crossing the blood–brain barrier (BBB) was an essential part of our chemistry design and presented its own challenges. Improving the BBB permeation of molecules has been widely studied and *in silico* prediction methods developed based on known CNS penetrant and nonpenetrant compounds.^{32,33} Examination of the physicochemical properties of molecules and their influence on affecting BBB permeability has suggested some guiding principles and a physicochemical property range to increase the probability of improving the BBB permeability.³³ The top 25% CNS penetrant drugs sold in 2004 were found to have mean values of PSA (Å²) 47, HBD 0.8, cLogP 2.8, cLogD (pH 7.4) 2.1, and MW 293. They suggested the following maximum limits when designing compounds as PSA < 90 Å², HBD < 3, cLogP 2–5, cLogD (pH 7.4) 2–5, MW < 500. As this was the first round of compound design, we restricted the compounds to the following parameters: PSA 40–70 Å², HBD < 3, cLogP 2–4.5, MW 250–400.

Virtual libraries of all possible compounds that could be constructed from our in-house chemical inventory were constructed and minimized to ensure that a wide region of chemical space was explored, and structures were not biased to one region. Reaction schemes, intermediates, and examples of compounds made are described in the [Supporting Information](#).

RESULTS AND DISCUSSION

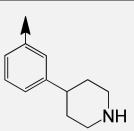
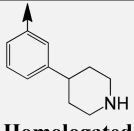
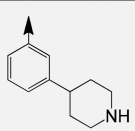
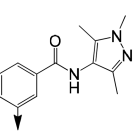
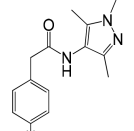
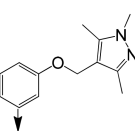
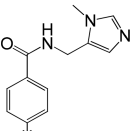
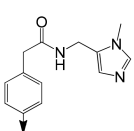
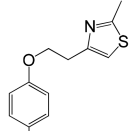
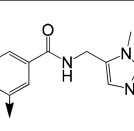
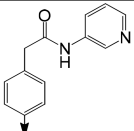
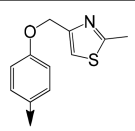
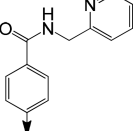
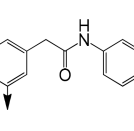
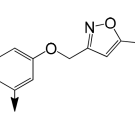
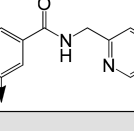
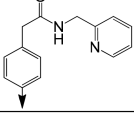
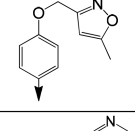
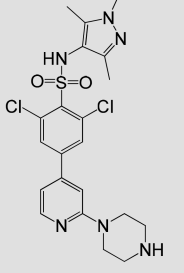
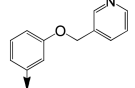
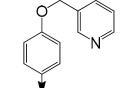
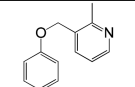
Scaffold Array Results. No compounds made in the Suzuki chemistry (1, Figure 3) derived series had a potency <10 μM against *Tb*NMT (see [Supporting Information](#) for compounds made). Table 1 shows the potency against *Tb*NMT for selected examples from the amide (3–7), homologated amide (8–12), and ether series (17–24). The most potent compound in the

amide series was 3 (*Tb*NMT IC₅₀ 1.7 μM). Amides directly linked to the phenyl ring in the 3-position were found to be more potent than the corresponding 4-substituted analogues (5 vs 4 and 7 vs 6). The homologated amide series in comparison to the amide series were on the whole >3-fold more potent (6 vs 12) with the most potent compound achieving a *Tb*NMT IC₅₀ value of 0.07 μM (10). In the homologated amides series the 4-position amides showed greater potency than the corresponding 3-position analogues (the opposite trend to the amide series). Further optimization of both the directly linked and homologated amide series failed to improve the potency or the pharmacokinetic properties.

The ether array produced compounds with good levels of activity against *Tb*NMT, the most active of these achieved an IC₅₀ value of 0.5 μM (24). The more potent compounds were substituted in the 4-position, on average showing around 10-fold greater potency over their 3-position analogues, e.g., 3-position compound 22 (35 μM) vs 4-position compound 23 (1.2 μM) or 3-position compound 20 (13 μM) vs 4-position compound 21 (1.4 μM). Interestingly, the replacement of the sulfonamide in structure 1 with an ether linkage (17) was completely inactive against *Tb*NMT (IC₅₀ > 100 μM). This was surprising, as methyl ethers are considered possible sulfonamide bioisosteres.³¹ Compound 24 was not selective over human NMT (*Hs*NMT1) but exhibited an EC₅₀ of 2 μM in the *T. br. brucei* proliferation assay, with good microsomal stability and moderate levels of selectivity against proliferating human MRC-5 cells (Figure 4).

The crystal structure of 24 bound to *Af*NMT (Figure 4A) shows the ligand binds in the peptide binding groove in an overall U-shaped conformation, with the ligand wrapping round the side chain of Phe157. The central aryl rings of 24 lie perpendicular to each other allowing the ligand to sit in the cleft formed by the side

Table 1. Array Chemistry Selected Results for the Amide, Homologated Amides, and Ether Series

	 Amides	<i>Tb</i> NMT IC ₅₀ (μ M) ^b		 Homologated Amides	<i>Tb</i> NMT IC ₅₀ (μ M) ^b		 Ether	<i>Tb</i> NMT IC ₅₀ (μ M) ^b
3 ^a		1.7	8*		0.4	17 ^a		>100
4*		>100	9*		0.60	18 ^a		9.5
5 ^a		15	10*		0.07	19 ^a		1.6
6 ^a		>100	11*		13	20 ^a		13
7 ^a		2.9	12*		0.60	21 ^a		1.4
1 ^a		0.002				22 ^a		35
						23 ^a		1.2
						24 ^a		0.5

*Compounds greater than 90% pure. ^aCompounds >95% pure. ^bIC₅₀ values are shown as mean values of two or more determinations. Standard deviation was typically within 2-fold from the IC₅₀. nd = not determined.

chain of Tyr263, Tyr393, and Leu436. The cleft is formed by the movement of the side chain of Tyr273; a feature observed in the binding mode of benzofuran ligands^{26,27} and subsequent derivatives.³⁴

The pyridyl nitrogen of **24** forms an interaction with Ser378 in a similar orientation as the trimethyl-pyrazole group of **1**, and the piperidine moiety interacts directly with the C-terminal carboxyl group of Leu492.

Compound **24** does not interact with His265, an interaction formed by the sulfonamide in **1** (overlaid with **24**, Figure 4B), which potentially explained the drop off in potency between **1** (*Tb*NMT 0.002 μ M) and **24** (0.5 μ M). Despite this loss of activity, **24** had comparable ligand efficiency (LE)³⁵ of 0.33 to **1**, LE = 0.36, and in combination with the observed binding mode, gave us confidence that the design strategy was valid.

Optimization of Compound 24. With the aim of increasing potency against *Tb*NMT, the diphenyl piperidine ring was replaced with the dichlorophenyl-pyridyl-piperidine moiety of **1**. This change reduced the logP by \sim 1 log unit from 4.3 for **24**, with an increase in PSA from 34 \AA^2 (19) to 50 \AA^2 , which was within the acceptable guidance limits for BBB permeability^{32,33} to give **29** (synthesis shown in Scheme 1).

Compound **29** (Figure 5) exhibited a 4-fold improvement in potency against *Tb*NMT (IC₅₀ 0.1 μ M) and improved efficacy in the *T. brucei* proliferation assay (EC₅₀ 0.7 μ M), while retaining good microsomal stability (1.4 mL/min/g) and LE (0.33). Encouragingly, **29** showed good levels of brain penetration (brain–blood = 0.4), a significant improvement over **1** (brain–blood < 0.1),²² indicating that the strategy of reducing MW and PSA was a valid approach (**1**, PSA 101 \AA , MW 495). The crystal structure of **29** bound to *Af*NMT (Figure 6) was determined

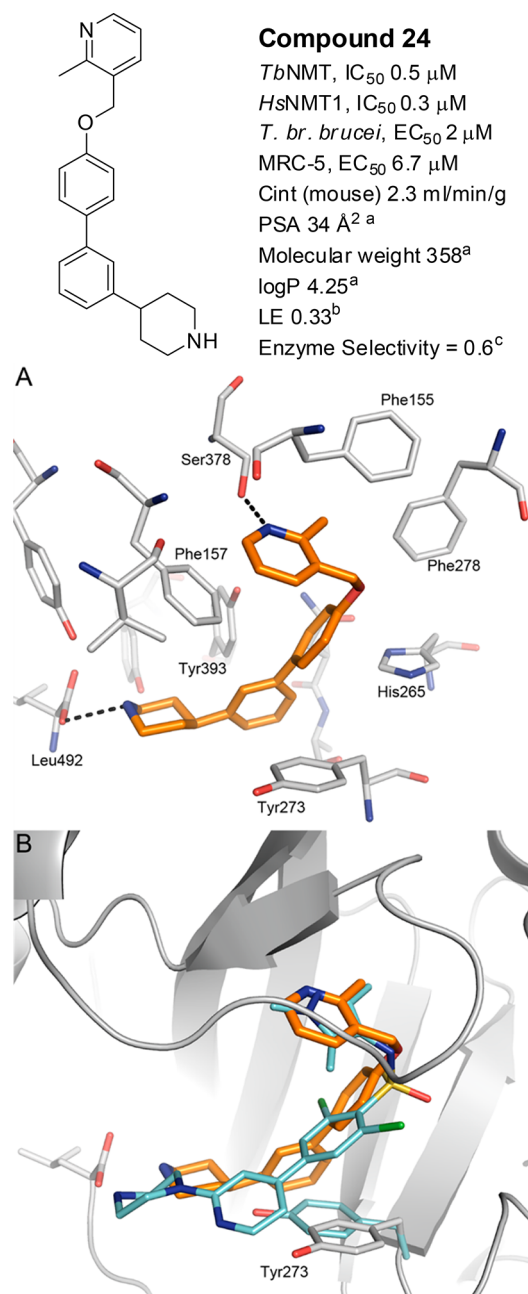


Figure 4. Binding mode of **24**. (A) Compound **24** (C atoms gold) bound to AfNMT (C atoms gray). PDB 5TSU. H-bonds are shown as dashed lines and key residues labeled. (B) Comparison of the binding mode of **24** with **1** bound to AfNMT (PDB 4CAX), highlighting the movement of Tyr273. Compound **1** and the side chain of Tyr273 (PDB 4CAX) are shown with cyan C atoms.

showing the ligand adopted a conformation similar to **1** with the biaryl system sitting in plane with the 2,6-dichlorophenyl ring stacking in plane with the side chain of Tyr273. Key interactions between the piperidine N to Ser378 and the piperazine to the C-terminal carboxyl group are retained from **24**.

Replacement of the 2,6-Dichlorophenyl Ring. Optimization of **29** focused on modifications to the central 2,6-dichlorophenyl ring to increase enzymatic selectivity relative to *Hs*NMT1 (0.3 μM, 3-fold compared to *Tb*NMT IC₅₀). These modifications were made employing the same chemistry as outlined in Scheme 1, by varying the starting substituted

bromophenol used in the Mitsunobu step. These 2,6-dichlorophenyl modifications are detailed in Table 2.

None of the core modifications improved potency against *Tb*NMT when compared to **29** (Table 2) nor LE and enzyme selectivity, although some demonstrated increased levels of potency against *Hs*NMT1 (**37**, *Hs*NMT1, IC₅₀ 0.01 μM). The reason for this increase in *Hs*NMT1 activity was not explained using the available crystal structure data. Certainly inhibitors of human NMT such as **37** are of potential interest in the treatment of cancer,²⁰ and further elaboration of the core could be explored.

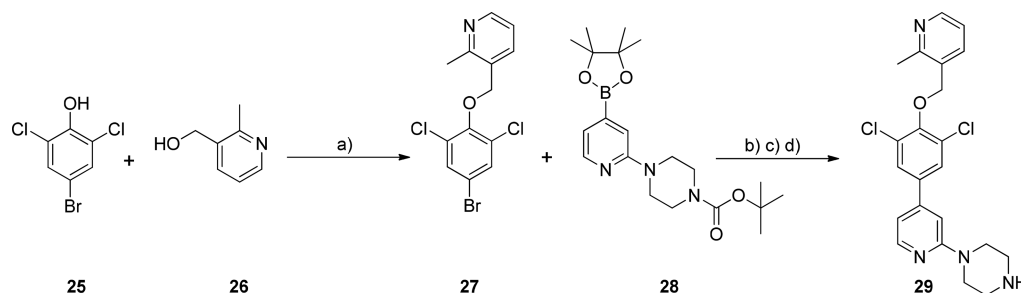
Pyridyl Headgroup SAR. The next phase of optimization focused on modifications to the ether pyridyl ring of **29** shown in Table 3. These compounds were made using the same common phenol intermediate (Scheme 2), applying solid phase reagents such as polystyrene bound triphenylphosphine, and running reactions and purifications in parallel using commercially available alcohols or alcohols derived from commercially available carboxylic acids or esters after reduction with borane or lithium aluminum hydride (see Supporting Information).

Modifications to the pyridyl headgroup showed encouraging results with **47** equipotent to **29** (IC₅₀ ≈ 0.1 μM) but with ~65-fold selectivity over *Hs*NMT1, equivalent activity in the *T. br. brucei* proliferation assay, and promising microsomal stability (C_{int} 4.2 mL/min/g). Compound **30**, though, had equivalent activity to **29** in the MRC-5 counter screen, indicating that *Hs*NMT1 activity may not have been driving the MRC-5 toxicity.

Homologation of the linker to the pyridyl group did not improve potency, as did groups on the pyridyl ring at the 6- (**48**) or 4-positions (**49**), though both **48** and **49** showed equivalent activity in the *T. br. brucei* proliferation assay to **29**. The crystal structure of **29** overlaid with the trimethylpyrazole of **1** suggested that additions of methyl substitution may have been beneficial to potency (Figure 7A) because the trimethyl substitution of pyrrole in **1** was essential for activity. Subsequent crystal structures of **48** showed that the binding pocket the pyridyl headgroup accesses is small and that these substituents in the case of **49** forced the ether pyridyl ring to twist in the pocket to avoid steric clashes with its dichlorophenyl ring, and for **48**, the 4-methyl forces the pyridyl ring out of the pocket. In both cases, the direct hydrogen bond from the pyridyl nitrogen to the serine was broken, but **48** still formed an interaction, though this was now water mediated (Figure 7B).

Alternative Nonpyridyl Head Group SARs. To advance the series, two regions within the structure were modified with the aim to improve potency, first examining pyridyl replacements and modifications to the pyridyl ring and replacement of the piperazino-pyridine moiety. First, the pyridyl ring was replaced with a range of five-membered heterocycles, mainly thiazoles, with various substitutions; see Table 4. The most potent of these showed levels of promising activity against *Tb*NMT (IC₅₀ ≈ 0.05–0.06 μM; **58** and **57**). The SAR around **57** was tight. The removal of either methyl groups (**60** and **65**) lost activity against *Tb*NMT; in addition, substitution of the 2-methyl group with either ethyl (**64**) or isopropyl (**66**) lost all activity in the *T. br. brucei* proliferation assay. Compound **57** showed good stability to microsomal turnover (C_{int} 2.4 mL/min/g) but also improved selectivity over MRC-5 cytotoxicity. Both **58** and **57** showed equivalent levels of potency against *Hs*NMT1 (IC₅₀ ≈ 0.03–0.08 μM) and again showed very different MRC-5 activities, indicating that MRC-5 toxicity may not be entirely driven by *Hs*NMT1 activity.

Replacement of the Piperazino-Pyridine Moiety. We had previously validated *Tb*NMT as a druggable target in the

Scheme 1^a

^aReagents and conditions: (a) polymer supported-PPh₃, DIAD, alcohol, THF; (b) dioxane/1 M aq K₃PO₄, Pd(PPh₃)₄; (c) TFA, DCM; (d) 2 M HCl in diethyl ether.

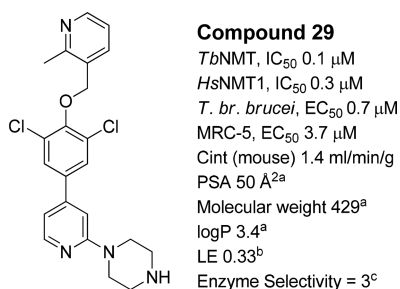


Figure 5. Compound 29 profile. ^aValues calculated using the Optibrium STARDROP software. ^bLigand efficiency (LE), calculated as 0.6·ln(IC₅₀)/(heavy atom count) using *T. brucei* NMT IC₅₀ potency. ^cIC₅₀ values are shown as mean values of two or more determinations. Standard deviation was typically within 2-fold from the IC₅₀. nd = not determined. ^dEnzyme selectivity calculated as *Hs*NMT1 IC₅₀ (μM)/*Tb*NMT IC₅₀ (μM).

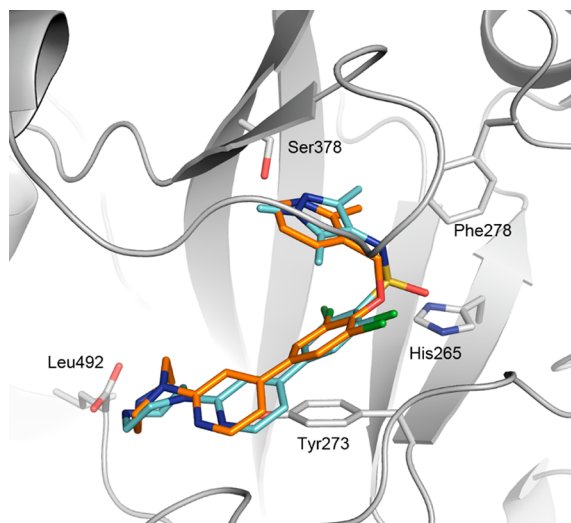


Figure 6. Binding mode of 29 (C atoms gold) bound to AfNMT (PDB 5T6C). Binding mode of 1 (C atoms cyan) is shown for comparison.

stage 2 model for HAT in mice using 68 as a model compound (Figure 8A).²⁴ Compound 68 showed good potency in the *T. br. brucei* proliferation assay at EC₅₀ 0.001 μM and improved levels of selectivity over MRC-5 cells when compared to 1. We examined hybridizing the 4-C chain derivative of 68, 69, which showed equally good efficacy and potency, and 29 to increase efficacy in the *T. br. brucei* proliferation assay. Compound 71 (synthesis in Scheme 3) showed increased selectivity over MRC-5 cells and *Hs*NMT1 but showed a significant drop off in efficacy

in the *T. br. brucei* proliferation assay. This was potentially caused by the significant increase in lipophilicity of 71 (logP 5.5) compared to 29 (logP 3.4), resulting in an increased level of nonspecific protein/membrane binding. Given the more favorable logP of 29, further optimization focused on derivatives of 29 rather than 71. Compound 70 (Scheme 3), the NH piperidine of 71, showed no *in vitro* activity against *Tb*NMT.

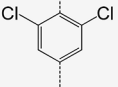
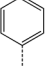
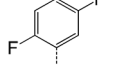
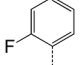
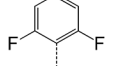
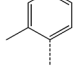
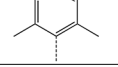
Pyridyl Headgroup Optimization. The crystal structure of 29 (Figure 6) indicated that the methyl substituent on the pyridyl ring was pointing into a small pocket. Chemistry was developed to explore this pocket with various hydrophobic and polar groups as detailed in Scheme 4. Using a common intermediate (ethyl 2-chloronicotinate, 72), Suzuki and Negishi reactions were used to install aromatics rings (73) and alkyl groups (74a–c), respectively. Amines were installed through displacement of the chlorine of 72. After reduction of the ethyl esters (73–75) to the corresponding alcohols (76–78), they were reacted using standard Mitsunobu conditions (Scheme 2) to give final products detailed in Table 5.

Good levels of inhibition of *Tb*NMT were observed for all compounds prepared (except 79), some with improved potency over 29. The loss of activity of 79 was most probably caused by the alkoxy-group reducing the basicity of the pyridine ring, making the ring nitrogen a poorer HBA. Compounds 81 and 82 showed promising potency against the parasite (EC₅₀ = 0.1 μM), with good selectivity compared to MRC-5 cells (81), and had good microsomal stability (81, 1.2 mL/min/mg; 82, 1.6 mL/min/mg). Compound 81 (Figure 9) showed significant levels of brain penetration (brain–blood ratio = 1.9), a significant improvement on 29 (brain–blood ratio 0.4) and 1 (brain–blood ratio < 0.1). Compound 81 represents a good lead for further optimization to identify development candidates for stage 2 HAT.

CONCLUSIONS

By using 1 as a starting point to identify alternative *Tb*NMT inhibitor scaffolds with physicochemical properties suitable for penetration into the brain to treat stage 2 HAT, we identified an ether linker as a replacement of the sulfonamide of 1. This modification reduced molecular weight and polar surface area, producing a viable alternative series with excellent levels of brain penetration. This work highlights the importance of decreasing the PSA as a way of increasing the probability of brain penetration. Further optimization identified compounds with good levels of *Tb*NMT and *T. br. brucei* antiproliferative activity and microsomal stability. Though in comparison with the original structure 1, further potency gains against the enzyme and in the parasite proliferation assay are required. This series

Table 2. Modifications to the 2,6-Dichlorophenyl Central Ring of Compound 29

	R	<i>Tb</i> NMT IC ₅₀ (μM) ^a	<i>Hs</i> NMT1 IC ₅₀ (μM) ^a	<i>T.br.</i> <i>brucei</i> Tryps EC ₅₀ (μM)	MRC- 5 EC ₅₀ (μM)	LE ^b	Enzyme Selectivity ^c
29		0.1	0.3	0.7	3.7	0.33	3
36		0.6	0.09	2.8	5.0	0.31	0.15
37		0.8	0.01	2.2	1.5	0.29	0.01
38		1.2	0.06	2.4	3.3	0.29	0.05
39		2.0	0.03	2.8	2.5	0.27	0.02
40		2.0	0.08	2.2	8.7	0.28	0.04
41		16	1.8	2.7	8.9	0.23	0.11

^aIC₅₀ values are shown as mean values of two or more determinations. Standard deviation was typically within 2-fold from the IC₅₀. nd = not determined. ^bLigand efficiency (LE), calculated as 0.6·ln(IC₅₀)/(heavy atom count) using *T. brucei* NMT IC₅₀ potency.²⁵ ^cEnzyme selectivity calculated as *Hs*NMT1 IC₅₀ (μM)/*Tb*NMT IC₅₀ (μM).

presents good leads to identify potential development candidates for stage 2 HAT.

EXPERIMENTAL SECTION

Synthetic Materials and Methods. Chemicals and solvents were purchased from the Aldrich Chemical Co., Fluka, ABCR, VWR, Acros, Fisher Chemicals, and Alfa Aesar and were used as received unless otherwise stated. Air- and moisture-sensitive reactions were carried out under an inert atmosphere of argon in oven-dried glassware. Analytical thin-layer chromatography (TLC) was performed on precoated TLC plates (layer 0.20 mm silica gel 60 with fluorescent indicator UV254, from Merck). Developed plates were air-dried and analyzed under a UV lamp (UV254/365 nm). Flash column chromatography was performed using prepacked silica gel cartridges (230–400 mesh, 40–63 μm, from SiliCycle) using a Teledyne Presearch ISCO Combiflash Companion 4X or Combiflash Retrieve. ¹H NMR and ¹³C NMR spectra were recorded on a Bruker Avance II 500 spectrometer (¹H at 500.1 MHz, ¹³C at 125.8 MHz) or a Bruker DPX300 spectrometer (¹H at 300.1 MHz). Chemical shifts (δ) are expressed in ppm recorded using the residual solvent as the internal reference in all cases. Signal splitting patterns are described as singlet (s), doublet (d), triplet (t), quartet (q), pentet (p), multiplet (m), broad (br), or a combination thereof. Coupling constants (*J*) are quoted to the nearest 0.1 Hz. LC–MS analyses were performed with either an Agilent HPLC 1100 series connected to a Bruker Daltonics micrOTOF or an Agilent Technologies 1200 series HPLC connected to an Agilent Technologies 6130 quadrupole LC–MS, where both instruments were connected to an Agilent diode array detector. LC–MS chromatographic separations were conducted with a Waters Xbridge C18 column, 50 mm × 2.1 mm,

3.5 μm particle size; mobile phase, water/acetonitrile + 0.1% HCOOH, or water/acetonitrile + 0.1% NH₃; linear gradient 80:20 to 5:95 over 3.5 min, and then held for 1.5 min; flow rate 0.5 mL min⁻¹. All assay compounds had a measured purity of ≥95% (by TIC and UV) as determined using this analytical LC–MS system; a lower purity level is indicated. High-resolution electrospray measurements were performed on a Bruker Daltonics MicrOTOF mass spectrometer. Microwave-assisted chemistry was performed using a Biotage Initiator Microwave Synthesizer.

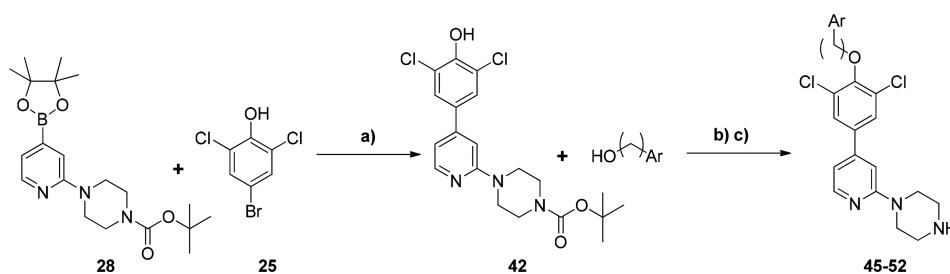
tert-Butyl-4-(3-Bromophenyl)piperidine-1-carboxylate (14). A solution of 4-(3-bromophenyl)piperidine-hydrochloride (**13**) (5.1 g, 18.4 mmol, 1 equiv), Boc₂O (4.4 g, 20.2 mmol, 1.1 equiv), and triethylamine (3.87 mL, 27.8 mmol, 1.5 equiv) in THF (50 mL) was stirred at room temperature for 16 h. The reaction was filtered, and the filtrate was washed with dilute 10% citric acid and extracted into ethyl acetate. The ethyl acetate layer was washed with water, then dried over MgSO₄, filtered, and evaporated to give an off-white solid (**14**) (6.13 g, 98% yield). ¹H NMR, 500 MHz, CDCl₃ δ1.51 (s, 9H), 1.57–1.66 (m, 2H), 1.81–1.86 (m, 2H), 2.64 (tt, *J* = 3.70, 12.21, 1H), 2.77–2.85 (m, 2H), 4.22–4.32 (m, 2H), 7.14–7.22 (m, 2H), 7.35–7.39 (m, 2H). [M + H]⁺ = 388.4.

tert-Butyl 4-(3'-Hydroxy-[1,1'-biphenyl]-3-yl)piperidine-1-carboxylate (15). *tert*-Butyl 4-(3-bromophenyl)piperidine-1-carboxylate (**14**) (2 g, 5.88 mmol, 1 equiv), 3-hydroxyphenyl boronic acid (974 mg, 7.06 mmol, 1.2 equiv), anhydrous dioxane (10 mL), and 1 M aq K₃PO₄ (6 mL) were combined in a microwave vessel and argon bubbled through the mixture for 5 min. Pd(PPh₃)₄ (136 mg, 0.118 mmol, 2%), was added, and the reaction was degassed again for a further 5 min before microwaving at 140 °C for 15 min. The resulting solution was extracted into dichloromethane, washed with sat. aq NaHCO₃, and passed

Table 3. Pyridyl Head Group SAR of Compound 29

	R	<i>Tb</i> NMT IC ₅₀ (μM) ^a	<i>Hs</i> NMT1 IC ₅₀ (μM) ^a	<i>T. br.</i> <i>brucei</i> Tryps EC ₅₀ (μM)	MRC- 5 EC ₅₀ (μM)	LE ^b	Enzyme Selectivity ^c
29		0.1	0.3	0.7	3.7	0.33	3
45		5.4	>1	>25	>1	0.26	nd
46		1.6	0.1	>1	>1	0.28	0.67
47		0.1	6.5	0.4	4.6	0.34	65
48		0.8	1.3	0.6	2.8	0.28	1.6
49		0.3	0.2	0.5	2.3	0.31	0.7
50		0.8	>1	>1	>1	0.29	nd
51		1.3	0.5	>10	>1	0.28	0.4
52		4.6	0.7	>10	>1	0.25	0.15

^aIC₅₀ values are shown as mean values of two or more determinations. Standard deviation was typically within 2-fold from the IC₅₀. nd = not determined. ^bLigand efficiency (LE), calculated as 0.6·ln(IC₅₀)/(heavy atom count) using *T. brucei* NMT IC₅₀ potency.²⁵ ^cEnzyme selectivity calculated as *Hs*NMT1 IC₅₀ (μM)/*Tb*NMT IC₅₀ (μM).

Scheme 2⁴⁴

^aReagents and conditions: (a) Boc₂O, NEt₃, THF; (b) 4-bromo-2,6-dichlorophenol, MeCN/1 M aq K₃PO₄, Pd(dppf)₂Cl₂, (c) PS-PPh₃, DIAD, alcohol, THF; (d) TFA, DCM.

through a phase separation cartridge. The organic layer was then absorbed onto silica and purified by flash column chromatography running a gradient from 0% ethyl acetate/hexane to 50% ethyl acetate/hexane to give **15** as a colorless oil (1.76 g, 85% yield). ¹H NMR 500 MHz, CDCl₃ δ 1.53 (s, 9H), 1.60–1.76 (m, 2H), 1.83–1.91 (m, 2H), 2.71 (tt, *J* = 3.68, 12.33, 1H), 2.70–2.91 (m, 2H), 4.24–4.32 (br. s, 2H), 5.02 (s, 1H), 6.96–6.99 (m, 2H), 7.18–7.21 (m, 1H), 7.39–7.48 (m, 3H), 7.52–7.56 (m, 2H). [M + H]⁺ = 354.2331, 298.1651 (product – ^tBu).

tert-Butyl 4-(4'-Hydroxy-[1,1'-biphenyl]-3-yl)piperidine-1-carboxylate (**16**). A mixture of 4-hydroxyphenylboronic acid (183 mg, 1.32 mmol, 1 equiv), *tert*-butyl 4-(3-bromophenyl)piperidine-1-carboxylate (**14**) (450 mg, 1.32 mmol, 1 equiv), Pd(PPh₃)₄ (30 mg), and K₃PO₄ (1

equiv) in DMF–H₂O (3:1, 4 mL) afforded **16** (326 mg, 70% yield). ¹H NMR 500 MHz, DMSO, δ 1.56 (s, 9H), 1.68–1.74 (m, 2H), 1.86–1.96 (m, 2H), 2.72–2.80 (m, 1H), 2.80–3.00 (m, 2H), 4.29–4.32 (br. s, 2H), 5.02 (s, 1H), 6.96–6.99 (m, 2H), 7.18–7.21 (m, 1H), 7.39–7.48 (m, 3H), 7.52–7.56 (m, 2H). [M + H]⁺ = 354.2331, 298.1651 (product – ^tBu).

4-(3'-((1,3,5-Trimethyl-1H-pyrazol-4-yl)methoxy)-[1,1'-biphenyl]-3-yl)piperidine (**17**). *tert*-Butyl 4-(3'-hydroxy-[1,1'-biphenyl]-3-yl)piperidine-1-carboxylate (**15**) (100 mg, 0.28 mmol, 1 equiv), (1,3,5-trimethylpyrazole)methanol (44 mg, 0.31 mmol, 1.1 equiv), polystyrene bound-PPh₃ (PPh₃ = triphenylphosphine, 1.84 mmol/g loading, 228

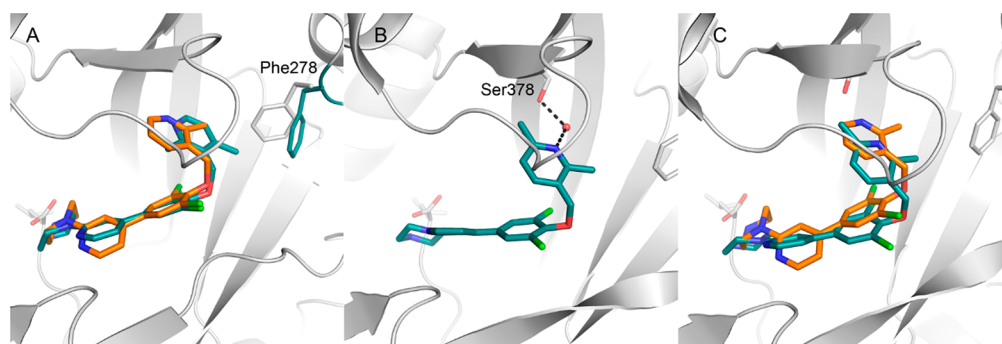


Figure 7. Binding mode of pyridyl headgroup modifications. (A) Binding mode of **49** (C atoms aquamarine; PDB 5T6H) compared with **29** (C atoms gold). The side chain of Phe278 rotates to accommodate the 4-methyl group. (B) Binding mode of **48** (C atoms aquamarine; PDB 5T6E); the interaction with Ser378 is now a water bridged interaction. (C) Compound **48** compared with **29**.

mg, 0.42 mmol, 1.5 equiv), diisopropyl azodicarboxylate (DIAD, 66 μ L, 0.34 mmol, 1.2 equiv) in anhydrous dioxane (5 mL) in a capped test tube was heated at 60 $^{\circ}$ C for 16 h. The reaction was absorbed onto silica and purified by flash column chromatography running a gradient from 0% ethyl acetate/hexane to 100% ethyl acetate. The resulting product was evaporated *in vacuo* before dissolving in dichloromethane (10 mL), addition of trifluoroacetic acid (10 equiv) and stirring at RT for 3 h. The reaction was then evaporated *in vacuo* before dissolving in dichloromethane and loading onto a prewashed SCX cartridge. The SCX cartridge was washed with dichloromethane (3 \times 10 mL) and MeOH (3 \times 10 mL) before eluting the product with 7 N ammonia in methanol. This was evaporated to give **17** (64 mg, 61% yield). ^1H NMR 500 MHz, CDCl_3 , δ 1.66 (s, 3H), 1.67–1.75 (m, 2H), 1.87–1.92 (m, 2H), 2.70–2.77 (m, 1H), 2.80–2.89 (m, 2H), 3.76 (s, 3H), 4.22–4.35 (m, 2H), 4.90 (s, 2H), 6.39 (br. s, 1H), 6.98–7.01 (m, 1H), 7.20–7.23 (m, 3H), 7.37–7.47 (m, 4H). $[\text{M} + \text{H}]^+ = 427.2$.

Compounds **14–20** were made in an analogous manner to **17** from **16**, see Supporting Information for analytical data.

Prototypical Mitsunobu Reaction of a Pyridyl Alcohol and a Substituted Phenol (Scheme 1). See Supporting Information for the synthesis of intermediates **30–35** for compounds **36–41** (Table 2).

3-((4-Bromo-2,6-dichlorophenoxy)methyl)-2-methylpyridine (27). DIAD (diisopropyl azodicarboxylate, 5 mL, 24.8 mmol, 1.2 equiv) was added to a suspension of 4-bromo-2,6-dichlorophenol (**25**) (5.0 g, 20.7 mmol, 1 equiv), 2-methyl-3-hydroxymethylpyridine (**26**) (3.1 g, 24.8 mmol, 1.2 equiv), and polystyrene bound- PPh_3 (1.84 mmol/g loading, 16.2 g, 29.8 mmol, 1.2 equiv) in anhydrous THF (20 mL) then heated at 70 $^{\circ}$ C for 4 h. After cooling, the reaction mixture was filtered, the beads washed with MeOH and dichloromethane, and the filtrate concentrated *in vacuo*. The resulting residue was triturated with MeOH to give **27** as a white solid (5.46 g, 76% yield). ^1H NMR 500 MHz, CDCl_3 , δ 2.68 (s, 3H), 5.03 (s, 2H), 7.18 (dd, $J = 4.90, 7.68$ Hz, 1H), 7.49 (s, 3H), 7.82 (dd, $J = 1.68, 7.68$ Hz, 1H), 8.50 (dd, $J = 1.68, 4.90$ Hz, 1H). LC–MS $[\text{M} + \text{H}]^+ = 347.9$.

tert-Butyl 4-(4-(4,4,5,5-Tetramethyl-1,3,2-dioxaborolan-2-yl)pyridin-2-yl)piperazine-1-carboxylate (28). A solution of 1-(4-(4,4,5,5-tetramethyl-1,3,2-dioxaborolan-2-yl)pyridin-2-yl)piperazine (2.97 g, 10.27 mmol, 1 equiv), *di-tert-butyl*-dicarbonate (Boc_2O , 2.5 g, 11.3 mmol, 1.1 equiv), in THF (20 mL) and triethylamine (2.1 mL, 15.4 mmol, 1.5 equiv) was stirred at RT overnight. The resulting reaction was extracted into dichloromethane, and then washed with 10% citric acid and then water. The dichloromethane layer was dried over MgSO_4 , filtered and evaporated to give (**28**) as a white solid (4 g, 100% yield). ^1H NMR 500 MHz, CDCl_3 , δ 1.28 (s, 12H), 1.42 (s, 9H), 3.45–3.50 (m, 8H), 6.90 (d, $J = 4.91$, 1H), 6.97 (s, 1H), 8.14 (dd, $J = 1.02, 4.89$, 1H). $[\text{M} + \text{H}]^+ = 389.45$.

Prototypical Suzuki Reaction of an Aryl Bromide and a Boronate Ester (Compounds 29–35). 1-(4-(3,5-Dichloro-4-((2-methylpyridin-3-yl)methoxy)phenyl)pyridin-2-yl)piperazine Dihydrochloride Salt (**29**). *tert-Butyl* 4-(4-(4,4,5,5-tetramethyl-1,3,2-dioxaborolan-2-yl)pyridin-2-yl)piperazine-1-carboxylate (**28**) (67 mg, 0.23 mmol, 1 equiv), 3-((4-bromo-2,6-dichlorophenoxy)methyl)-2-methylpyridine (**27**) (80 mg, 0.23 mmol, 1 equiv), and potassium phosphate-trihydrate

(49 mg, 0.231 mmol, 1 equiv) in $\text{DMF-H}_2\text{O}$ (1:1, 4 mL) was combined in a microwave vessel and degassed with argon for 5 min, before the addition of $\text{Pd}(\text{PPh}_3)_4$ (14 mg, 0.012 mmol, 5%), and reaction degassed again, then microwaved at 100 $^{\circ}$ C for 40 min. Reaction was concentrated *in vacuo*, extracted into dichloromethane, and then washed with aq NaHCO_3 . The two-phase system was passed through a phase separation cartridge, the filtrate concentrated *in vacuo*, and the title compound purified by flash column chromatography using 8% MeOH/ethyl acetate + 1% aq NH_3 as the eluent. The residue was taken up in dichloromethane, ethereal HCl was added (2 M, 2 mL) and concentrated, and the dihydrochloride salt of **29** was triturated with ether, filtered, and washed with ether (104 mg, 71% yield). ^1H NMR 500 MHz, d_6 -DMSO δ 2.82 (s, 3H), 3.17–3.23 (m, 4H), 3.85–3.90 (m, 4H), 5.29 (s, 2H), 7.16 (d, $J = 5.20$ Hz, 1H), 7.27–7.30 (m, 1H), 7.78–7.86 (m, 1H), 8.06 (s, 2H), 8.22 (d, $J = 5.20$ Hz, 1H), 8.41–8.51 (m, 1H), 8.71–8.77 (m, 1H), 9.15 (br s, 2H). HRMS $[\text{M} + \text{H}]^+$ calculated for $\text{C}_{22}\text{H}_{23}\text{Cl}_2\text{N}_4\text{O}_1 = 429.1243$, found = 429.1240.

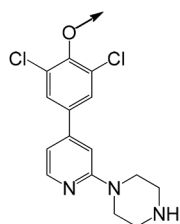
1-(4-(4-((2-Methylpyridin-3-yl)methoxy)phenyl)pyridin-2-yl)piperazine Dihydrochloride Salt (36). Prepared from 3-((4-bromophenoxy)methyl)-2-methylpyridine (**30**) (150 mg, 0.54 mmol, 1 equiv) and 1-(4-(4,4,5,5-tetramethyl-1,3,2-dioxaborolan-2-yl)pyridin-2-yl)piperazine (**28**) (156 mg, 0.54 mmol, 1 equiv), according to the method outlined for the synthesis of **29**, to give **36** as a dihydrochloride salt (150 mg, 64% yield). ^1H NMR 500 MHz, DMSO δ 2.79 (s, 2H), 3.21–3.27 (m, 4H), 3.93–3.98 (m, 4H), 5.40 (s, 2H), 7.21–7.30 (m, 3H), 7.35–7.43 (m, 1H), 7.86–7.95 (m, 3H), 8.15 (d, $J = 6.00$ Hz, 1H), 8.53 (d, $J = 7.45$ Hz, 1H), 8.74 (d, $J = 5.75$ Hz, 1H), 9.39 (br s, 2H). LC–MS $[\text{M} + \text{H}]^+ = 361.2$. HRMS $[\text{M} + \text{H}]^+$ calculated for $\text{C}_{22}\text{H}_{25}\text{N}_4\text{O}_1 = 361.2023$, found = 361.2033.

1-(4-(2,5-Difluoro-4-((2-methylpyridin-3-yl)methoxy)phenyl)pyridin-2-yl)piperazine Dihydrochloride (37). Prepared from 3-((4-bromo-2,5-difluorophenoxy)methyl)-2-methylpyridine (**31**) (106 mg, 0.34 mmol, 1 equiv) and **28** (98 mg, 0.34 mmol, 1 equiv), according to the method outlined for the synthesis of **29**, to give **37** as a dihydrochloride salt (124 mg, 78% yield). ^1H NMR 500 MHz, DMSO δ 2.79 (s, 3H), 3.17–3.23 (m, 4H), 3.84–3.90 (m, 4H), 5.48 (s, 2H), 6.99–7.03 (m, 1H), 7.14–7.19 (m, 1H), 7.57 (dd, $J = 7.20, 12.20$ Hz, 1H), 7.75 (dd, $J = 7.33, 11.83$ Hz, 1H), 7.90 (t, $J = 7.90$ Hz, 1H), 8.20 (d, $J = 5.55$ Hz, 1H), 8.49 (d, $J = 7.25$ Hz, 1H), 8.76 (d, $J = 5.65$ Hz, 1H), 9.32 (br s, 2H). LC–MS $[\text{M} + \text{H}]^+ = 397.2$. HRMS $[\text{M} + \text{H}]^+$ calculated for $\text{C}_{22}\text{H}_{23}\text{F}_2\text{N}_4\text{O}_1 = 397.1834$, found = 397.1848.

1-(4-(2-Fluoro-4-((2-methylpyridin-3-yl)methoxy)phenyl)pyridin-2-yl)piperazine Dihydrochloride (38). Prepared from 3-((4-bromo-3-fluorophenoxy)methyl)-2-methylpyridine (**32**) (100 mg, 0.34 mmol, 1 equiv) and **28** (98 mg, 0.34 mmol, 1 equiv), according to the method outlined for the synthesis of **29**, to give **38** as a dihydrochloride salt (110 mg, 72% yield). ^1H NMR 500 MHz, DMSO δ 2.81 (s, 3H), 3.19–3.25 (m, 4H), 3.89–3.96 (m, 4H), 5.42 (s, 2H), 7.02–7.08 (m, 1H), 7.13 (dd, $J = 1.85, 8.35$ Hz, 1H), 7.25 (dd, $J = 1.63, 12.88$ Hz, 1H), 7.70 (t, $J = 8.65$ Hz, 1H), 7.92 (t, $J = 6.48$ Hz, 1H), 8.17 (d, $J = 5.65$ Hz, 1H), 8.55 (d, $J = 7.65$ Hz, 1H), 8.75 (d, $J = 5.05$ Hz, 1H), 9.47 (br s, 2H). LC–MS

Table 4. Pyridyl Head Group Replacements

	R	<i>Tb</i> NMT IC ₅₀ (μM) ^a	<i>Hs</i> NMT1 IC ₅₀ (μM) ^a	<i>T. br.</i> <i>brucei</i> Tryps EC ₅₀ (μM)	MRC- 5 EC ₅₀ (μM)	LE ^b	Enzyme Selectivity ^c
		0.1	0.3	0.7	3.7	0.33	3
		0.3	4.4	1.1	3.5	0.32	15
		0.05	0.08	0.33	2.2	0.34	2
		0.06	0.03	0.8	>10	0.34	0.5
		2.9	>100	>100	>100	0.34	>34
		1.3	15	2.8	3.1	0.26	11
		0.3	14	>10	>10	0.29	46
		0.5	9.9	>100	>1	0.33	20
		0.2	0.9	>1	>100	0.33	5
		0.3	0.3	>100	>1	0.30	1
		2.0	0.9	>100	>1	0.29	0.5
		3.5	3.8	>15	2.0	0.24	1
		4.2	12	>10	>10	0.24	3



^aIC₅₀ values are shown as mean values of two or more determinations. Standard deviation was typically within 2-fold from the IC₅₀. nd = not determined. ^bLigand efficiency (LE), calculated as 0.6·ln(IC₅₀)/(heavy atom count) using *T. brucei* NMT IC₅₀ potency.²⁵ ^cEnzyme selectivity calculated as *Hs*NMT1 IC₅₀ (μM)/*Tb*NMT IC₅₀ (μM).

[M + H]⁺ = 379.2. HRMS [M + H]⁺ calculated for C₂₂H₂₄F₂N₄O₁ = 379.1929, found = 379.1942.

1-(4-(2,6-Difluoro-4-((2-methylpyridin-3-yl)methoxy)phenyl)pyridin-2-yl)piperazine Dihydrochloride (**39**). Prepared from 3-((4-bromo-3,5-difluorophenoxy)methyl)-2-methylpyridine (**33**) (106 mg, 0.34 mmol, 1 equiv) and **28** (98 mg, 0.34 mmol, 1 equiv), according to the method outlined for the synthesis of **29**, to give **39** as a dihydrochloride salt (109 mg, 69% yield). ¹H NMR 500 MHz, DMSO δ 2.77 (s, 3H), 3.16–3.21 (m, 4H), 3.77–3.82 (m, 4H), 5.40 (s, 2H), 6.82 (d, *J* = 4.95 Hz, 1H), 7.03–7.07 (m, 1H), 7.14 (d, *J* = 9.90 Hz, 2H), 7.86–7.91 (m, 1H), 8.23 (d, *J* = 5.20 Hz, 1H), 8.49 (d, *J* = 6.30 Hz, 1H), 8.75 (d, *J* = 5.45 Hz, 1H), 9.20 (br s, 2H). LC–MS [M + H]⁺ =

397.2. HRMS [M + H]⁺ calculated for C₂₂H₂₃F₂N₄O₁ = 397.1834, found = 397.1852.

1-(4-(2-Methyl-4-((2-methylpyridin-3-yl)methoxy)phenyl)pyridin-2-yl)piperazine Dihydrochloride (**40**). Prepared from 3-((4-bromo-3-methylphenoxy)methyl)-2-methylpyridine (**34**) (150 mg, 0.51 mmol, 1 equiv) and **28** (148 mg, 0.51 mmol, 1 equiv), according to the method outlined for the synthesis of **29**, to give **40** as a dihydrochloride salt (110 mg, 48% yield). ¹H NMR 500 MHz, DMSO δ 2.29 (s, 3H), 2.77 (s, 3H), 3.17–3.23 (m, 4H), 3.83–3.88 (m, 4H), 5.34 (s, 2H), 6.80–6.84 (m, 1H), 6.96–7.00 (m, 1H), 7.04 (dd, *J* = 2.58, 8.43 Hz, 1H), 7.10 (d, *J* = 2.50 Hz, 1H), 7.25 (d, *J* = 8.45 Hz, 1H), 7.85 (t, *J* = 6.63 Hz, 1H), 8.15 (d, *J* = 5.80 Hz, 1H), 8.47 (d, *J* = 7.25 Hz, 1H), 8.72 (d, *J* = 5.20 Hz, 1H),

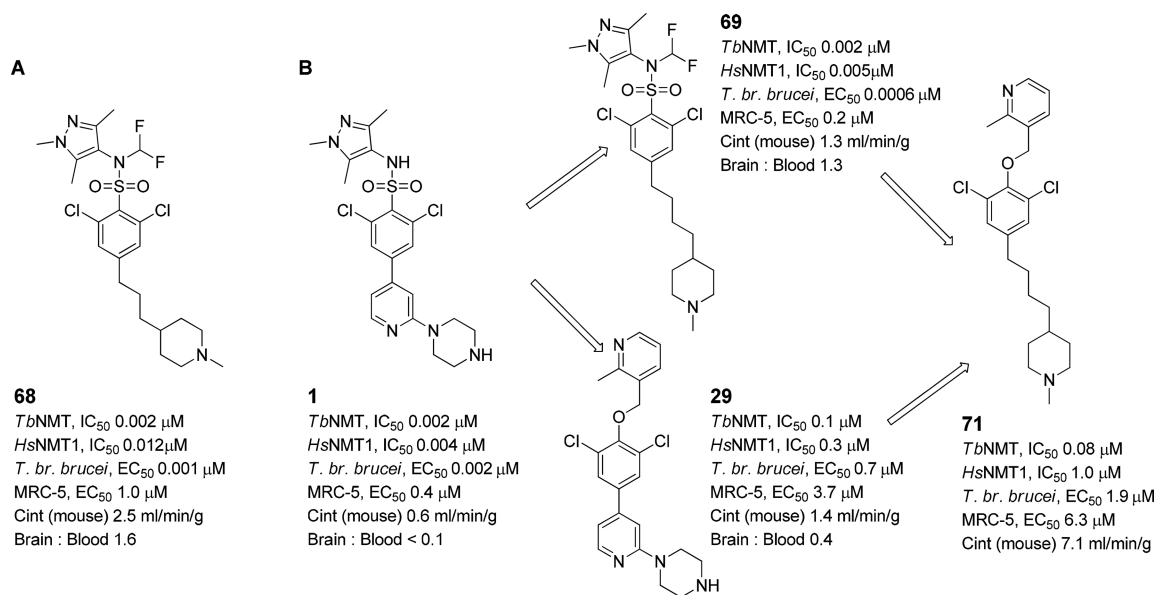
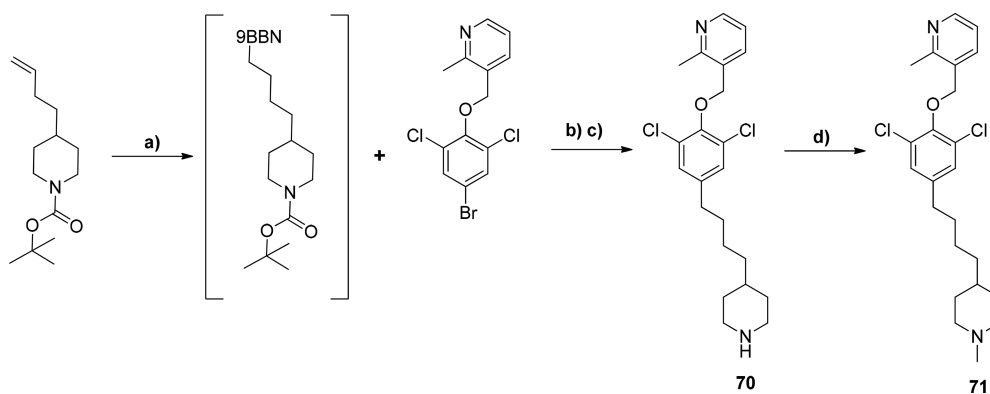
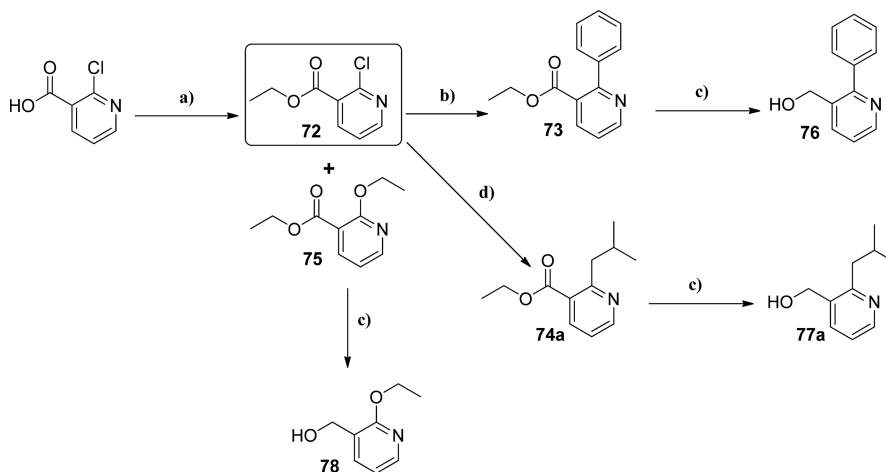


Figure 8. Hybridization approach.

Scheme 3^{aa}

^{aa}Reagents and conditions: (a) 9-BBN, THF; (b) Pd(PPh₃), K₃PO₄, H₂O, DMF; (c) TFA, DCM; (d) CH₂O, Na(OAc)₃BH, CHCl₃.

Scheme 4^{aa}

^{aa}Reagents and conditions: (a) H₂SO₄, EtOH; (b) phenylboronic acid, 1 M K₃PO₄/dioxane, Pd(PPh₃)₄; (c) 2 M LiAlH₄ in THF, 0 °C; (d) Pd(^tBuP)₂, 0.5 M isobutylzinc bromide, anhydrous THF.

9.27 (br s, 2H). LC-MS [M + H]⁺ = 375.2. HRMS [M + H]⁺ calculated for C₂₃H₂₇N₄O₁ = 375.2179, found = 375.2191.

1-(4-(2,6-Dimethyl-4-((2-methylpyridin-3-yl)methoxy)phenyl)-pyridin-2-yl)piperazine Dihydrochloride (**41**). Prepared from 3-((4-

Table 5. Pyridyl Substitutions

	R	<i>Tb</i> NMT IC ₅₀ (μM) ^a	<i>Hs</i> NMT1 IC ₅₀ (μM) ^a	<i>T. brucei</i> EC ₅₀ (μM)	MRC-5 EC ₅₀ (μM)	LE ^b	Enzyme Selectivity ^c
29		0.1	0.3	0.7	3.7	0.33	3
79		>50	>50	>50	>50		
80		0.1	0.04	>10	14	0.28	0.4
81		0.02	0.04	0.1	1.5	0.33	2
82		0.08	0.2	0.1	2.1	0.28	3
83		0.02	0.04	0.3	>1	0.34	2
84		0.06	0.18	0.5	1.4	0.29	3

^aIC₅₀ values are shown as mean values of two or more determinations. Standard deviation was typically within 2-fold from the IC₅₀. nd = not determined. ^bLigand efficiency (LE), calculated as 0.6·ln(IC₅₀)/(heavy atom count) using *T. brucei* NMT IC₅₀ potency.²⁵ ^cEnzyme selectivity calculated as *Hs*NMT1 IC₅₀ (μM)/*Tb*NMT IC₅₀ (μM).

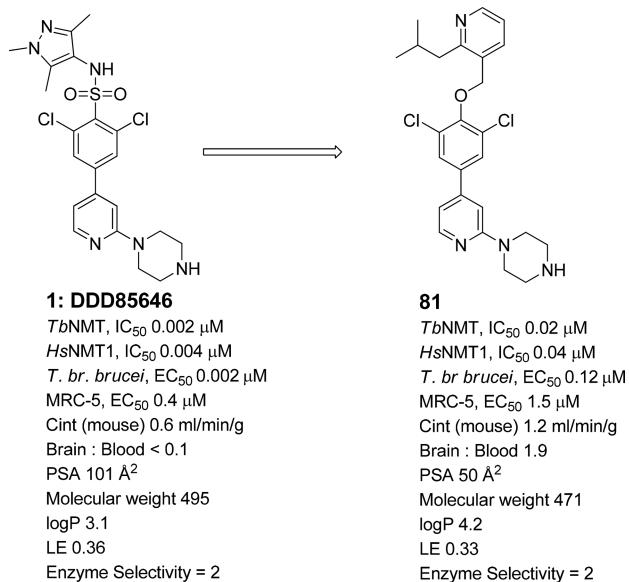


Figure 9. Comparison of 1 and 81.

bromo-3,5-dimethylphenoxy)methyl)-2-methylpyridine (35) (150 mg, 0.49 mmol, 1 equiv) and 28 (142 mg, 0.49 mmol, 1 equiv), according to the method outlined for the synthesis of 29, to give 41 as a dihydrochloride salt (177 mg, 75% yield). ¹H NMR 500 MHz,

DMSO δ 2.033 (s, 6H), 2.79 (s, 3H), 3.17–3.23 (m, 4H), 3.84–3.89 (m, 4H), 5.31 (s, 2H), 6.63–6.67 (m, 1H), 6.89–6.93 (m, 3H), 7.89 (t, *J* = 6.70 Hz, 1H), 8.18 (d, *J* = 5.35 Hz, 1H), 8.51 (d, *J* = 7.70 Hz, 1H), 8.73 (dd, *J* = 1.10, 5.65 Hz, 1H), 9.36 (br s, 2H). LC–MS [*M* + *H*]⁺ = 389.2. HRMS [*M* + *H*]⁺ calculated for C₂₄H₂₉N₄O₁ = 389.2336, found = 389.2335.

tert-Butyl 4-(4-(3,5-Dichloro-4-hydroxyphenyl)pyridin-2-yl)-piperazine-1-carboxylate (42). A solution of a *tert*-butyl 4-(4-(4,4,5,5-tetramethyl-1,3,2-dioxaborolan-2-yl)pyridin-2-yl)piperazine-1-carboxylate 28 (2.0 g, 5.14 mmol, 1.2 equiv), and 4-bromo-2,6-dichlorophenol (25) (1.04 g, 4.3 mmol, 1 equiv) in acetonitrile (7 mL) and aq 1 M K₃PO₄ (5 mL) was degassed by bubbling argon through for 5 min; then Pd(dppf)₂Cl₂ (175 mg, 0.22 mmol, 5%) was added and the reaction degassed again for a further 5 min before microwaving at 100 °C for 30 min. The cooled solution was diluted with dichloromethane and washed with aq NaHCO₃, the dichloromethane layer was dried over MgSO₄, and the filtrate was evaporated onto silica and purified by flash column chromatography running a gradient from 0% ethyl acetate/hexane to 50% ethyl acetate/hexane to give 42 as a white solid (1.07 g, 49% yield). ¹H NMR 500 MHz, CDCl₃ δ 1.52 (s, 9H), 3.58–3.64 (m, 8H), 6.05 (br s, 1H), 6.72 (s, 1H), 6.79 (d, *J* = 5.30, 1H), 7.53 (s, 2H), 8.25 (d, *J* = 5.19, 1H). [*M* + *H*]⁺ = 424.2.

1-(4-(3,5-Dichloro-4-(2-(pyridin-3-yl)ethoxy)phenyl)pyridin-2-yl)-piperazine (51). Diisopropyl azodicarboxylate (DIAD, 61 μL, 0.31 mmol, 1.1 equiv) was added to a suspension of 2-(pyridin-3-yl)ethanol (42 mg, 0.34 mmol, 1.2 equiv), polystyrene bound-PPh₃ (1.84 mmol/g loading, 200 mg, 0.37 mmol, 1.2 equiv), and 42 (120 mg, 0.28 mmol, 1 equiv) in anhydrous THF (20 mL) and then heated at 70 °C for 4 h. After cooling, the reaction mixture was filtered, the beads washed with

MeOH and dichloromethane, and the filtrate absorbed onto silica and purified by flash column chromatography running a gradient from 0% ethyl acetate/hexane to 100% ethyl acetate. The resulting residue was dissolved in dichloromethane (10 mL), trifluoroacetic acid (10 equiv) was added, and the reaction was stirred at RT for 16 h. The reaction was evaporated *in vacuo* before loading onto a prewashed SCX cartridge. The cartridge was washed with dichloromethane (3 × 10 mL) and MeOH (3 × 10 mL) before eluting with 7 N ammonia in methanol. This was absorbed onto silica and purified by flash column chromatography running a gradient from 0% MeOH/dichloromethane + 1% NH₃ to 20% MeOH/dichloromethane + 1% NH₃ to give **51** as a white solid (35 mg, 29% yield). ¹H NMR 500 MHz, CDCl₃ δ 3.02–3.05 (m, 4H), 3.22 (t, J = 6.90 Hz, 2H), 3.58–3.61 (m, 4H), 4.30 (t, J = 6.90 Hz, 2H), 6.71 (s, 1H), 6.75 (dd, J = 1.50, 5.25 Hz, 1H), 7.28–7.31 (m, 1H), 7.52 (s, 2H), 7.72–7.74 (m, 1H), 8.25 (dd, J = 0.61, 5.24 Hz, 1H), 8.54 (dd, J = 1.61, 4.97 Hz, 1H), 8.63 (d, J = 2.11 Hz, 1H). [M + H]⁺ = 429.1. HRMS [M + H]⁺ calculated for C₂₂H₂₃Cl₂N₄O₁ = 429.1243, found = 429.1245.

1-(4-(3,5-Dichloro-4-(pyridin-4-ylmethoxy)phenyl)pyridin-2-yl)piperazine (45). Prepared using **42** (120 mg, 0.28 mmol, 1 equiv) and pyridin-4-ylmethanol (37 mg, 0.34 mmol, 1.2 equiv), according to the Mitsunobu reaction and BOC deprotection procedure outlined for the synthesis **51**, to give **45** as an off-white solid (1 mg, 1% yield). ¹H NMR 500 MHz, CDCl₃ δ 3.04–3.06 (m, 4H), 3.61–3.63 (m, 4H), 5.14 (s, 2H), 6.74 (s, 1H), 6.78 (dd, J = 1.52, 5.39 Hz, 1H), 7.52–7.53 (m, 2H), 7.58 (s, 2H), 8.28 (d, J = 5.25 Hz, 1H), 8.69 (dd, J = 1.80, 5.94 Hz, 2H). [M + H]⁺ = 415.1.

1-(4-(3,5-Dichloro-4-(pyridin-3-ylmethoxy)phenyl)pyridin-2-yl)piperazine (46). Prepared using **42** (120 mg, 0.28 mmol, 1 equiv) and pyridin-3-ylmethanol (33 μL, 0.34 mmol, 1.2 equiv), according to the Mitsunobu reaction and BOC deprotection procedure outlined for the synthesis **51**, to give **46** as an off-white solid (17 mg, 15% yield). ¹H NMR 500 MHz, CDCl₃ δ 3.06–3.11 (m, 4H), 3.63–3.67 (m, 4H), 5.15 (s, 2H), 6.74 (s, 1H), 6.79 (s, 1H), 7.37–7.41 (m, 1H), 7.55–7.58 (m, 2H), 7.96–7.99 (m, 1H), 8.26–8.28 (m, 1H), 8.64–8.67 (m, 1H), 8.77–8.80 (m, 1H). [M + H]⁺ = 415.2. HRMS [M + H]⁺ calculated for C₂₁H₂₁Cl₂N₄O₁ = 415.1087, found = 415.1079.

1-(4-(3,5-Dichloro-4-(pyridin-2-ylmethoxy)phenyl)pyridin-2-yl)piperazine (47). Prepared using **42** (186 mg, 0.44 mmol, 1 equiv) and pyridin-2-ylmethanol (58 mg, 0.53 mmol, 1.2 equiv), according to the Mitsunobu reaction and BOC deprotection procedure outlined for the synthesis **51**, to give **47** as an off-white solid (130 mg, 71% yield). ¹H NMR 500 MHz, CDCl₃ δ 3.04–3.06 (m, 4H), 3.60–3.63 (m, 4H), 5.25 (s, 2H), 6.74 (d, J = 5.29 Hz, 1H), 6.78 (s, 1H), 7.29 (d, J = 1.26 Hz, 2H), 7.30–7.32 (m, 1H), 7.80–7.86 (m, 2H), 8.27 (d, J = 5.25 Hz, 1H), 8.63 (d, J = 4.30 Hz, 1H). [M + H]⁺ = 415.1. HRMS [M + H]⁺ calculated for C₂₁H₂₁Cl₂N₄O₁ = 415.1087, found = 415.1088.

1-(4-(3,5-Dichloro-4-((2,6-dimethylpyridin-3-yl)methoxy)phenyl)pyridin-2-yl)piperazine (48). Prepared using **42** (200 mg, 0.44 mmol, 1 equiv) and (2,6-dimethylpyridin-3-yl)methanol (**43**) (for synthesis see [Supporting Information](#)) (78 mg, 0.57 mmol, 1.2 equiv), according to the Mitsunobu reaction and BOC deprotection procedure outlined for the synthesis **51**, to give **48** as an off-white solid (130 mg, 63% yield). ¹H NMR 500 MHz, CDCl₃ δ 2.59 (s, 3H), 2.72 (s, 3H), 3.0–3.07 (m, 4H), 3.60–3.63 (m, 4H), 5.11 (s, 2H), 6.74 (s, 1H), 6.78 (d, J = 5.27 Hz, 1H), 7.07 (d, J = 7.81 Hz, 1H), 7.57 (s, 2H), 7.76 (d, J = 7.81 Hz, 1H), 8.27 (d, J = 5.16 Hz, 1H). [M + H]⁺ = 443.1. HRMS [M + H]⁺ calculated for C₂₃H₂₅Cl₂N₄O₁ = 443.14, found = 443.1402.

1-(4-(3,5-Dichloro-4-((2,4-dimethylpyridin-3-yl)methoxy)phenyl)pyridin-2-yl)piperazine (49). Prepared using **42** (112 mg, 0.28 mmol, 1 equiv) and (2,6-dimethylpyridin-4-yl)methanol (**44**) (for synthesis see [Supporting Information](#)) (44 mg, 0.32 mmol, 1.2 equiv), according to the Mitsunobu reaction and BOC deprotection procedure outlined for the synthesis **51**, to give **49** as an off-white solid (56 mg, 49% yield). ¹H NMR 500 MHz, DMSO δ 2.44 (s, 3H), 2.68 (s, 3H), 2.93–2.99 (m, 4H), 3.60–3.68 (m, 4H), 5.24 (s, 2H), 7.00 (d, J = 5.20 Hz, 1H), 7.10–7.14 (m, 2H), 7.96 (s, 2H), 8.16 (d, J = 5.1 Hz, 1H), 8.29 (d, J = 5.13 Hz, 1H). [M + H]⁺ = 443.2. HRMS [M + H]⁺ calculated for C₂₃H₂₅Cl₂N₄O₁ = 443.1400, found = 443.1392.

1-(4-(3,5-Dichloro-4-(2-(pyridin-2-yl)ethoxy)phenyl)pyridin-2-yl)piperazine (50). Prepared using **42** (120 mg, 0.28 mmol, 1 equiv) and 2-

(2-hydroxyethyl)pyridine (38 μL, 0.34 mmol, 1.2 equiv), according to the Mitsunobu reaction and BOC deprotection procedure outlined for the synthesis **51**, to give **50** as an off-white solid (24 mg, 20% yield). ¹H NMR 500 MHz, CDCl₃ δ 3.02–3.05 (m, 4H), 3.39 (t, J = 6.75 Hz, 2H), 3.58–3.61 (m, 4H), 4.49 (t, J = 6.65 Hz, 2H), 6.71 (s, 1H), 6.75 (dd, J = 1.50 Hz, 5.25 Hz, 1H), 7.18–7.21 (m, 1H), 7.39 (d, J = 7.93 Hz, 1H), 7.51 (s, 2H), 7.65–7.69 (m, 1H), 8.25 (dd, J = 0.64, 5.25 Hz, 1H), 8.58–8.60 (m, 1H). [M + H]⁺ = 429.1. HRMS [M + H]⁺ calculated for C₂₂H₂₃Cl₂N₄O₁ = 429.1243, found = 429.1231.

1-(4-(3,5-Dichloro-4-(2-(pyridin-4-yl)ethoxy)phenyl)pyridin-2-yl)piperazine (52). Prepared using **42** (112 mg, 0.28 mmol, 1 equiv) and 4-(2-hydroxyethyl)pyridine (42 mg, 0.34 mmol, 1.2 equiv) according to the Mitsunobu reaction and BOC deprotection procedure outlined for the synthesis **51**, to give **52** as an off-white solid (22 mg, 18% yield). ¹H NMR 500 MHz, CDCl₃ δ 3.02–3.05 (m, 4H), 3.22 (t, J = 6.68 Hz, 2H), 3.58–3.61 (m, 4H), 4.33 (t, J = 6.68 Hz, 2H), 6.71 (s, 1H), 6.75 (dd, J = 1.44 Hz, 5.25 Hz, 1H), 7.33 (dd, J = 1.59, 5.96 Hz, 2H), 7.53 (s, 2H), 8.25 (dd, J = 0.57, 5.19 Hz, 1H), 8.58 (dd, J = 1.54, 4.22 Hz, 2H). [M + H]⁺ = 429.1. HRMS [M + H]⁺ calculated for C₂₂H₂₃Cl₂N₄O₁ = 429.123956, found = 429.123956.

Compounds **56–57** were synthesized using the standard Mitsunobu coupling conditions followed by BOC deprotection using TFA from **42** according to the procedure outlined in the synthesis of **51** or, in the case of **56**, using the methodology used for compound **29**.

3-((2,6-Dichloro-4-(2-(piperazin-1-yl)pyridin-4-yl)phenoxy)methyl)-5-methylisoxazole Dihydrochloride (56). 4-Bromo-2,6-dichlorophenol (500 mg, 2.07 mmol, 1 equiv) and (5-methylisoxazol-3-yl)methanol (351 mg, 3.10 mmol, 1.5 equiv) were reacted according to the method outlined for **27** to give 3-((4-bromo-2,6-dichlorophenoxy)methyl)-5-methylisoxazole as a white solid (348 mg, 50% yield). ¹H NMR 500 MHz, CDCl₃ δ 2.46 (d, J = 0.85 Hz, 3H), 5.08 (s, 2H), 6.28–6.29 (m, 1H), 7.48 (s, 2H). LC–MS [M + H]⁺ = 337.9.

3-((4-Bromo-2,6-dichlorophenoxy)methyl)-5-methylisoxazole (100 mg, 0.30 mmol, 1 equiv) and 28 (86 mg, 0.30 mmol, 1 equiv) were reacted according to the method outlined for the synthesis of 29 to give 56 as a dihydrochloride salt (104 mg, 71% yield). ¹H NMR 300 MHz, DMSO δ 2.45 (s, 3H), 3.17–3.26 (m, 4H), 3.90–3.97 (m, 4H), 5.14 (s, 2H), 6.48–6.50 (m, 1H), 7.24 (d, J = 6.03 Hz, 1H), 7.37–7.40 (m, 1H), 8.07 (s, 2H), 8.20 (d, J = 5.73 Hz, 1H), 9.36 (br s, 2H). LC–MS [M + H]⁺ = 419.1. HRMS [M + H]⁺ calculated for C₂₀H₂₁N₄O₂Cl₂ = 419.1042, found = 419.1032.

5-((2,6-Dichloro-4-(2-(piperazin-1-yl)pyridin-4-yl)phenoxy)methyl)-2,4-dimethylthiazole (57). Prepared using **42** (200 mg, 0.47 mmol, 1 equiv) and (2,4-dimethyl-1,3-thiazol-5-yl)methanol (82 mg, 0.57 mmol, 1.2 equiv), according to the Mitsunobu reaction and BOC deprotection procedure outlined for the synthesis of **51**, to give **57** as an off-white solid (70 mg, 36% yield). ¹H NMR 500 MHz, CDCl₃ δ 2.46 (s, 3H), 2.71 (s, 3H), 3.04–3.07 (m, 4H), 3.61–3.64 (m, 4H), 5.19 (s, 2H), 6.73 (s, 1H), 6.77 (d, J = 5.27 Hz, 1H), 7.56 (s, 2H), 8.26 (d, J = 5.27 Hz, 1H). [M + H]⁺ = 449.0913. HRMS [M + H]⁺ calculated for C₂₁H₂₃Cl₂N₄O₁S₁ = 449.0964, found = 449.0949.

5-((2,6-Dichloro-4-(2-(piperazin-1-yl)pyridin-4-yl)phenoxy)methyl)-2,4-dimethylisoxazole (58). Prepared using **42** (120 mg, 0.28 mmol, 1 equiv) and (2,4-dimethylisoxazol-5-yl)methanol (**51**) (see [Supporting Information](#) for synthesis) (53 mg, 0.42 mmol, 1.5 equiv), according to the Mitsunobu reaction and BOC deprotection procedure outlined for the synthesis of **51**, to give **58** as an off-white solid (20 mg, 17% yield). ¹H NMR 500 MHz, CDCl₃ δ 2.09 (s, 3H), 2.47 (s, 3H), 3.03–3.06 (m, 4H), 3.60–3.63 (m, 4H), 5.10 (s, 2H), 6.72 (s, 1H), 6.77 (dd, J = 1.28, 5.11 Hz, 1H), 7.54 (s, 2H), 8.26 (d, J = 5.18 Hz, 1H). [M + H]⁺ = 433.2. HRMS [M + H]⁺ calculated for C₂₁H₂₃Cl₂N₄O₂ = 433.1193, found = 433.1200.

4-((2,6-Dichloro-4-(2-(piperazin-1-yl)pyridin-4-yl)phenoxy)methyl)-2,5-dimethylisoxazole (59). Prepared using **42** (120 mg, 0.28 mmol, 1 equiv) and (2,5-dimethyl-1,3-oxazol-4-yl)methanol (53 mg, 0.42 mmol, 1.5 equiv), according to the Mitsunobu reaction and BOC deprotection procedure outlined in the synthesis of **51**, to give **59** as an off-white solid (27 mg, 22% yield). ¹H NMR 500 MHz, CDCl₃ δ 2.37 (s, 3H), 2.46 (s, 3H), 3.03–3.06 (m, 4H), 3.60–3.62 (m, 4H), 4.97 (s, 2H),

6.73 (s, 1H), 6.77 (dd, $J = 1.53, 5.21$ Hz, 1H), 7.55 (s, 2H), 8.26 (dd, $J = 0.61, 5.21$ Hz, 1H). $[M + H]^+ = 433.1$.

4-((2,6-Dichloro-4-(2-(piperazin-1-yl)pyridin-4-yl)phenoxy)methyl)-2-methylthiazole (**60**). Prepared using **42** (150 mg, 0.35 mmol, 1 equiv) and 2-(2-methyl-1,3-thiazol-4-yl)methanol (54 mg, 0.42 mmol, 1.2 equiv), according to the Mitsunobu reaction and BOC deprotection procedure outlined for the synthesis of **51**, to give **60** as an off-white solid (15 mg, 10% yield). $^1\text{H NMR}$ 500 MHz, CDCl_3 δ 2.77 (s, 3H), 3.03–3.06 (m, 4H), 3.60–3.62 (m, 4H), 5.22 (s, 2H), 6.74 (s, 1H), 6.77 (dd, $J = 1.45, 5.10$ Hz, 1H), 7.37 (s, 1H), 7.56 (s, 2H), 8.26 (d, $J = 5.22$ Hz, 1H). $[M + H]^+ = 435.1$.

2-((2,6-Dichloro-4-(2-(piperazin-1-yl)pyridin-4-yl)phenoxy)methyl)thiazole (**61**). Prepared using **42** (120 mg, 0.28 mmol, 1 equiv) and 2-(hydroxymethyl)-1,3-thiazole (48 mg, 0.42 mmol, 1.5 equiv), according to the Mitsunobu reaction and BOC deprotection procedure outlined in the synthesis of **51**, to give **61** as an off-white solid (24 mg, 20% yield). $^1\text{H NMR}$ 500 MHz, CDCl_3 δ 3.03–3.06 (m, 4H), 3.60–3.62 (m, 4H), 5.44 (s, 2H), 6.73 (s, 1H), 6.77 (dd, $J = 1.41, 5.14$ Hz, 1H), 7.48 (d, $J = 3.30$ Hz, 1H), 7.57 (s, 2H), 7.86 (d, $J = 3.30$ Hz, 1H), 8.27 (d, $J = 3.30$ Hz, 1H). $[M + H]^+ = 423.1$. HRMS $[M + H]^+$ calculated for $\text{C}_{19}\text{H}_{19}\text{Cl}_2\text{N}_4\text{O}_1\text{S}_1 = 421.0651$, found = 421.0641.

4-((2,6-Dichloro-4-(2-(piperazin-1-yl)pyridin-4-yl)phenoxy)methyl)thiazole (**62**). Prepared using **42** (120 mg, 0.28 mmol, 1 equiv) and 4-(hydroxymethyl)-1,3-thiazole (48 mg, 0.42 mmol, 1.5 equiv), according to the Mitsunobu reaction and BOC deprotection procedure outlined for the synthesis of **51**, to give **62** as an off-white solid (5 mg, 4% yield). $^1\text{H NMR}$ 500 MHz, CDCl_3 δ 3.03–3.06 (m, 4H), 3.60–3.62 (m, 4H), 5.34 (s, 2H), 6.74 (s, 1H), 6.78 (dd, $J = 1.47, 5.23$ Hz, 1H), 7.57 (s, 2H), 7.62–7.63 (m, 1H), 8.27 (dd, $J = 0.68, 5.13$ Hz, 1H), 8.87 (d, $J = 2.09$ Hz, 1H). $[M + H]^+ = 423.1$.

5-((2,6-Dichloro-4-(2-(piperazin-1-yl)pyridin-4-yl)phenoxy)methyl)-4-methylthiazole (**63**). Prepared using **42** (120 mg, 0.28 mmol, 1 equiv) and (4-methylthiazol-5-yl)methanol (**52**) (for synthesis, see Supporting Information) (54 mg, 0.42 mmol, 1.5 equiv), according to the Mitsunobu reaction and BOC deprotection procedure outlined for the synthesis of **51**, to give **63** as an off-white solid (9 mg, 7% yield). $^1\text{H NMR}$ 500 MHz, CDCl_3 δ 2.56 (s, 3H), 3.03–3.06 (m, 4H), 3.60–3.63 (m, 4H), 5.28 (s, 2H), 6.73 (s, 1H), 6.77 (dd, $J = 1.46, 5.19$ Hz, 1H), 7.57 (s, 2H), 8.27 (dd, $J = 0.6, 5.19$ Hz, 1H), 8.79 (s, 1H). $[M + H]^+ = 435.1$. HRMS $[M + H]^+$ calculated for $\text{C}_{20}\text{H}_{21}\text{Cl}_2\text{N}_4\text{O}_1\text{S}_1 = 435.0808$, found = 435.0809.

5-((2,6-Dichloro-4-(2-(piperazin-1-yl)pyridin-4-yl)phenoxy)methyl)-2-ethyl-4-methylthiazole (**64**). Prepared using **42** (120 mg, 0.28 mmol, 1 equiv) and (2-ethyl-4-methyl-1,3-thiazol-5-yl)methanol (66 mg, 0.42 mmol, 1.5 equiv), according to the Mitsunobu reaction and BOC deprotection procedure outlined for the synthesis of **51**, to give **64** as an off-white solid (26 mg, 20% yield). $^1\text{H NMR}$ 500 MHz, CDCl_3 δ 1.41 (t, $J = 7.81, 3\text{H}$), 2.47 (s, 3H), 3.00–3.06 (m, 6H), 3.60–3.62 (m, 4H), 5.19 (s, 2H), 6.73 (s, 1H), 6.77 (dd, $J = 1.42, 5.20$ Hz, 1H), 7.56 (s, 2H), 8.26 (d, $J = 5.13$ Hz, 1H). $[M + H]^+ = 463.1$. HRMS $[M + H]^+$ calculated for $\text{C}_{22}\text{H}_{25}\text{Cl}_2\text{N}_4\text{O}_1\text{S}_1 = 463.1121$, found = 463.1124.

5-((2,6-Dichloro-4-(2-(piperazin-1-yl)pyridin-4-yl)phenoxy)methyl)thiazole (**65**). Prepared using **42** (120 mg, 0.28 mmol, 1 equiv) and 5-(hydroxymethyl)-1,3-thiazole (48 mg, 0.42 mmol, 1.5 equiv), according to the Mitsunobu reaction and BOC deprotection procedure outlined for the synthesis of **51**, to give **65** as an off-white solid (23 mg, 20% yield). $^1\text{H NMR}$ 500 MHz, CDCl_3 δ 3.06–3.08 (m, 4H), 3.64–3.66 (m, 4H), 5.33 (s, 2H), 6.73 (s, 1H), 6.78 (dd, $J = 1.45, 5.20$ Hz, 1H), 7.56 (s, 2H), 7.96 (s, 1H), 8.27 (d, $J = 5.37$ Hz, 1H), 8.90 (s, 1H). $[M + H]^+ = 421.1$, 423.1. HRMS $[M + H]^+$ calculated for $\text{C}_{19}\text{H}_{19}\text{Cl}_2\text{N}_4\text{O}_1\text{S}_1 = 421.0651$, found = 421.064.

5-((2,6-Dichloro-4-(2-(piperazin-1-yl)pyridin-4-yl)phenoxy)methyl)-2-isopropyl-4-methylthiazole (**66**). Prepared using **42** (120 mg, 0.28 mmol, 1 equiv) and (2-isopropyl-4-methylthiazol-5-yl)methanol (**53**) (for synthesis, see Supporting Information) (73 mg, 0.42 mmol, 1.5 equiv), according to the Mitsunobu reaction and BOC deprotection procedure outlined for the synthesis of **51**, to give **66** as an off-white solid (37 mg, 28% yield). $^1\text{H NMR}$ 500 MHz, CDCl_3 δ 1.42 (d, $J = 7.12$ Hz, 6H), 2.48 (s, 2H), 3.03–3.06 (m, 4H), 3.31 (sept, $J = 6.97$ Hz, 1H), 3.60–3.63 (m, 4H), 5.19 (s, 2H), 6.73 (s, 1H), 6.77 (dd, $J =$

1.36, 5.23 Hz, 1H), 7.57 (s, 2H), 8.27 (dd, $J = 0.68, 5.23$ Hz, 1H). $[M + H]^+ = 477.2$. HRMS $[M + H]^+$ calculated for $\text{C}_{23}\text{H}_{27}\text{Cl}_2\text{N}_4\text{O}_1\text{S}_1 = 477.1277$, found = 477.1273.

4-((2,6-Dichloro-4-(2-(piperazin-1-yl)pyridin-4-yl)phenoxy)methyl)-2-isopropylthiazole (**67**). Prepared using **42** (120 mg, 0.28 mmol, 1 equiv) and 4-(hydroxymethyl)-2-isopropylthiazole (66 mg, 0.42 mmol, 1.5 equiv), according to the Mitsunobu reaction and BOC deprotection procedure outlined for the synthesis of **51**, to give **67** as an off-white solid (1 mg, 1% yield). $^1\text{H NMR}$ 500 MHz, CDCl_3 δ 1.43 (d, $J = 6.85$ Hz, 6H), 3.03–3.05 (m, 4H), 3.36 (sept, $J = 6.95$ Hz, 1H), 3.60–3.62 (m, 4H), 5.26 (s, 2H), 6.74 (s, 1H), 6.78 (dd, $J = 1.47, 5.18$ Hz, 1H), 7.55 (s, 2H), 8.26 (d, $J = 5.12$ Hz, 1H). $[M + H]^+ = 463.1$.

3-((2,6-Dichloro-4-(3-(piperidin-4-yl)propyl)phenoxy)methyl)-2-methylpyridine (**70**). To a solution of *tert*-butyl 4-(but-3-en-1-yl)piperidine-1-carboxylate (0.58 g, 2.4 mmol, 2 equiv) under argon in anhydrous THF (1 mL) was added 9-BBN (5.1 mL (0.5 M in THF), 2.55 mmol, 2.1 equiv), and the reaction was heated to 90 °C for 1 h in a microwave. To this crude reaction, 3-((4-bromo-2,6-dichlorophenoxy)methyl)-2-methylpyridine (0.42 g, 1.2 mmol, 1 equiv) and K_3PO_4 (1 M in H_2O , 2.4 mmol, 2 equiv) in anhydrous DMF (2.5 mL) was added and then degassed with argon. $\text{Pd}(\text{PPh}_3)_4$ (0.024 mmol, 28 mg, 2%) was then added, and the solution was microwaved at 110 °C for 1 h. The reaction was extracted into dichloromethane, washed with water, and dried over MgSO_4 . The crude material was purified by flash column chromatography, running a gradient from 0% ethyl acetate in hexane to 50% ethyl acetate in hexane. The Boc protected **70** was taken up in dichloromethane (12 mL), trifluoroacetic acid added (6 mL), and the reaction stirred for 2 h. The solvent was removed *in vacuo* to give a crude residue, which was purified by SCX-2, eluting with methanol to 2 M methanolic ammonia, followed by column chromatography, eluting with dichloromethane to dichloromethane–methanol (80:20) with 1% NH_3 , to give **70** (0.105 g, 10%) as an oil. $^1\text{H NMR}$ 500 MHz, CDCl_3 δ 1.05–1.13 (m, 2H), 1.23–1.40 (m, 5H), 1.58–1.62 (m, 7H), 2.57 (dd, $J = 7.7, 7.7$ Hz, 2H), 2.70 (s, 3H), 4.07–4.10 (m, 2H), 5.05 (s, 2H), 7.16 (s, 2H), 7.21 (dd, $J = 4.9, 7.6$ Hz, 1H), 7.90 (dd, $J = 1.5, 7.6$ Hz, 1H), 8.52 (dd, $J = 1.7, 4.9$ Hz, 1H). HRMS $[M + H]^+$ calculated for $\text{C}_{22}\text{H}_{23}\text{Cl}_2\text{N}_4\text{O} = 429.124343$, found = 429.124407.

3-((2,6-Dichloro-4-(3-(1-methylpiperidin-4-yl)propyl)phenoxy)methyl)-2-methylpyridine (**71**). 3-((2,6-Dichloro-4-(3-(piperidin-4-yl)propyl)phenoxy)methyl)-2-methylpyridine (**70**) (0.07 g, 0.17 mmol, 1 equiv) was taken up in chloroform (10 mL), treated with paraformaldehyde (0.052 g, 10 equiv), and heated at 55 °C for 1 h. The reaction mixture was then treated with sodium triacetoxyborohydride (0.183 g, 0.86 mmol, 5 equiv), and heating continued for 16 h. The reaction mixture was cooled to room temperature and then partitioned between dichloromethane and sodium bicarbonate solution. The dichloromethane layer was separated and dried over MgSO_4 and solvent removed. The crude material was purified by column chromatography, eluting with dichloromethane to dichloromethane–methanol (95:5) with 1% NH_3 , to give **71** as a white solid (58 mg, 76% yield). $^1\text{H NMR}$ 500 MHz, CDCl_3 δ 1.23–1.30 (m, 5H), 1.34–1.39 (m, 2H), 1.87–1.92 (m, 2H), 2.27 (s, 3H), 2.56 (dd, $J = 7.8, 7.8$ Hz, 2H), 2.70 (s, 4H), 2.85 (d, $J = 11.3$ Hz, 2H), 5.05 (s, 2H), 5.33 (s, 1H), 7.16 (s, 2H), 7.21 (dd, $J = 5.1, 7.6$ Hz, 1H), 7.90 (dd, $J = 1.6, 7.6$ Hz, 1H), 8.52 (dd, $J = 1.7, 4.8$ Hz, 1H). $[M + H]^+ = 421.1889$. HRMS $[M + H]^+$ calculated for $\text{C}_{23}\text{H}_{31}\text{Cl}_2\text{N}_2\text{O}_1 = 421.1808$, found = 421.1802.

Ethyl 2-Chloronicotinate (**72**) and Ethyl 2-Ethoxynicotinate (**75**). To a suspension of 2-chloronicotinic acid (4.6 g, 29.2 mmol) in ethanol (50 mL), conc. H_2SO_4 (2 mL) was added dropwise, and the suspension was heated to reflux for 3 h to form a solution. The reaction was then cooled and evaporated *in vacuo*, then carefully neutralized with sat. aq NaHCO_3 and extracted into ethyl acetate. The organic layer was washed with water and then dried over MgSO_4 , filtered, absorbed onto silica, and purified using flash column chromatography running a gradient from 0% ethyl acetate/hexane to 50% ethyl acetate/hexane, to give the title compounds (ethyl 2-chloronicotinate **72**, bottom spot, 2.33 g, 43% yield; ethyl 2-ethoxynicotinate **75**, top spot, 923 mg, 16% yield). Ethyl 2-chloronicotinate (**72**) $^1\text{H NMR}$ 500 MHz, CDCl_3 δ 1.45 (t, $J = 7.61$ Hz, 3H), 4.45 (q, $J = 7.07$ Hz, 2H), 7.36 (dd, $J = 4.76, 7.71$ Hz, 1H), 8.19 (dd, $J = 2.09, 7.87$ Hz, 1H), 8.54 (dd, $J = 2.09, 4.77$ Hz, 1H). $[M + H]^+ =$

186.1. Ethyl 2-ethoxynicotinate (**75**) ^1H NMR 500 MHz, CDCl_3 , δ 1.14 (t, $J = 7.06$ Hz, 3H), 1.47 (t, $J = 6.92$ Hz, 3H), 4.39 (q, $J = 7.20$ Hz, 2H), 4.50 (q, $J = 7.06$ Hz, 2H), 6.94 (dd, $J = 4.98, 7.48$ Hz, 1H), 8.16 (dd, $J = 2.01, 7.48$ Hz, 1H), 8.30 (dd, $J = 2.01, 4.88$ Hz, 1H). $[\text{M} + \text{H}]^+ = 196.1$.

Prototypical Negishi Reaction between a Chloropyridine and Alkylzinc Bromide. Ethyl 2-Isobutylnicotinate (74a). Anhydrous THF (9 mL) was added to a flame-dried argon purged flask containing ethyl 2-chloronicotinate (**72**) (227 mg, 1.2 mmol, 1 equiv) and $\text{Pd}(\text{tBuP})_2$ (31 mg, 0.06 mmol, 5%), and the mixture was stirred until clear. To this, isobutylzinc bromide (0.5 M in THF, 2.6 mL, 1.3 mmol, 1.1 equiv) was added dropwise, and the resulting solution was heated at 60 °C overnight. The reaction was absorbed onto silica and eluted to remove baseline material before purifying again by flash column chromatography using 25% ethyl acetate/hexane as the eluent, to give **74a** as a yellow oil (164 mg, 66% yield). ^1H NMR 500 MHz, CDCl_3 , δ 0.95 (d, $J = 6.75$ Hz, 6H), 1.43 (t, $J = 7.25$ Hz, 3H), 2.13 (sept, $J = 6.75$ Hz, 1H), 3.11 (d, $J = 7.25$ Hz, 2H), 4.41 (q, $J = 7.13$ Hz, 2H), 8.16 (dd, $J = 1.88, 7.75$ Hz, 1H), 8.67 (dd, $J = 1.88, 4.75$ Hz, 1H). $[\text{M} + \text{H}]^+ = 208$.

Prototypical Suzuki Reaction of a Chloropyridine and Boronic Acid. Ethyl 2-Phenylnicotinate (73). A solution of ethyl 2-chloronicotinate (**72**) (793 mg, 4.3 mmol, 1 equiv) and phenylboronic acid (773 mg, 6.4 mmol, 1.5 equiv) in 1 M aq K_3PO_4 (4 mL) and dioxane (6 mL) in a microwave vessel was degassed with argon for 5 min before addition of $\text{Pd}(\text{PPh}_3)_4$ (64 mg, 0.055 mmol, 5%) and degassing again for a further 5 min before microwaving at 140 °C for 15 min. The reaction mixture was partitioned between dichloromethane and sat. aq NaHCO_3 , and the organic layer was absorbed onto silica and purified by flash column chromatography running a gradient from 0% ethyl acetate/hexane to 25% ethyl acetate/hexane, affording **73** as an oil (927 mg, 95% yield). ^1H NMR 500 MHz, CDCl_3 , δ 1.07 (t, $J = 7.19$ Hz, 3H), 4.18 (q, $J = 7.19$ Hz, 2H), 7.37 (dd, $J = 4.91, 7.87$ Hz, 1H), 7.45–7.48 (m, 3H), 7.55–7.57 (m, 2H), 8.14 (dd, $J = 1.71, 7.76$ Hz, 1H), 8.79 (dd, $J = 1.83, 4.78$ Hz, 1H). $[\text{M} + \text{H}]^+ = 228.2$.

Prototypical Pyridyl Ester Reduction to an Alcohol. (2-Isobutylpyridin-3-yl)methanol (77a). To a solution of ethyl 2-isobutylnicotinate **74a** (774 mg, 3.7 mmol, 1 equiv) in anhydrous THF (5 mL) at 0 °C, 0.5 M LiAlH_4 in THF (5.6 mL, 11.2 mmol, 3 equiv) was added dropwise, and the solution was allowed to warm to room temperature before being stirred at rt for 16 h. Sodium sulfite decahydrate was added to the solution, and the reaction was diluted with dichloromethane and allowed to stir for 30 min. The reaction was filtered, the filtrate layers separated, and the organic layer dried over MgSO_4 and evaporated *in vacuo* to give **77a** as a yellow oil (452 mg, 74% yield). ^1H NMR 500 MHz, CDCl_3 , δ 0.97 (d, $J = 6.67$, 6H), 2.19 (sept, $J = 6.82$ Hz, 1H), 2.71 (d, $J = 7.42$ Hz, 2H), 4.79 (d, $J = 5.51$ Hz, 2H), 7.17 (dd, $J = 4.78, 7.82$ Hz, 1H), 7.60 (d, $J = 7.68$ Hz, 1H), 8.50 (dd, $J = 1.74, 4.78$ Hz, 1H). $[\text{M} + \text{H}]^+ = 166.2$.

1-(4-(3,5-Dichloro-4-((2-ethoxypyridin-3-yl)methoxy)phenyl)pyridin-2-yl)piperazine (79). Prepared using **42** (200 mg, 0.47 mmol, 1 equiv) and (2-ethoxypyridin-3-yl)methanol (**78**) (87 mg, 0.57 mmol, 1.2 equiv), according to the Mitsunobu reaction and BOC deprotection procedure outlined for the synthesis of **51**, to give **79** as an off-white solid (30 mg, 33% yield). ^1H NMR 500 MHz, CDCl_3 , δ 1.42 (t, $J = 7.21$ Hz, 3H), 2.66–2.69 (m, 4H), 3.65–3.68 (m, 4H), 4.41 (q, $J = 7.07$ Hz, 2H), 6.72 (dd, $J = 1.42, 5.21$ Hz, 1H), 6.90 (dd, $J = 5.04, 7.20$ Hz, 1H), 7.53 (s, 1H), 7.72 (dd, $J = 1.61, 7.50$ Hz, 1H), 8.09 (dd, $J = 1.96, 5.04$ Hz, 1H), 8.24 (d, $J = 5.24$ Hz, 1H). $[\text{M} + \text{H}]^+ = 459.2$. HRMS $[\text{M} + \text{H}]^+$ calculated for $\text{C}_{23}\text{H}_{25}\text{Cl}_2\text{N}_4\text{O}_2 = 459.1349$, found = 459.1339.

4-(3-((2,6-Dichloro-4-(2-(piperazin-1-yl)pyridin-4-yl)phenoxy)methyl)pyridin-2-yl)morpholine (80). Prepared using **42** (200 mg, 0.47 mmol, 1 equiv) and (2-morpholinopyridin-3-yl)methanol (110 mg, 0.57 mmol, 1.2 equiv), according to the Mitsunobu reaction and BOC deprotection procedure outlined for the synthesis of **51**, to give **80** as an off-white solid (58 mg, 28% yield). ^1H NMR 500 MHz, CDCl_3 , δ 3.04–3.06 (m, 4H), 3.28–3.31 (m, 4H), 3.60–3.63 (m, 4H), 3.88–3.90 (m, 4H), 5.15 (s, 2H), 6.74 (s, 1H), 6.79 (dd, $J = 1.48, 5.29$ Hz, 1H), 7.60 (s, 2H), 8.07 (dd, $J = 1.93, 7.51$ Hz, 1H), 8.28 (d, $J = 5.23$ Hz, 1H), 8.37 (dd, $J = 1.93, 4.89$ Hz, 1H). $[\text{M} + \text{H}]^+ = 500.2$. HRMS $[\text{M} + \text{H}]^+$ calculated for $\text{C}_{25}\text{H}_{28}\text{Cl}_2\text{N}_5\text{O}_2 = 500.161457$, found = 500.160771.

1-(4-(3,5-Dichloro-4-((2-isobutylpyridin-3-yl)methoxy)phenyl)pyridin-2-yl)piperazine (81). Prepared using **42** (200 mg, 0.47 mmol, 1 equiv) and (2-isobutylpyridin-3-yl)methanol (**77a**) (94 mg, 0.57 mmol, 1.2 equiv), according to the Mitsunobu reaction and BOC deprotection procedure outlined for the synthesis of **51**, to give **81** as an off-white solid (86 mg, 40% yield). ^1H NMR 500 MHz, CDCl_3 , δ 1.00 (d, $J = 6.69$ Hz, 6H), 2.23 (sept, $J = 6.91$ Hz, 1H), 3.04–3.06 (m, 4H), 3.60–3.63 (m, 4H), 5.14 (s, 2H), 6.74 (s, 1H), 6.78 (dd, $J = 1.44, 5.11$ Hz, 1H), 7.23 (dd, $J = 4.75, 7.63$ Hz, 1H), 7.59 (s, 2H), 7.98 (dd, $J = 1.73, 7.77$ Hz, 1H), 8.28 (dd, $J = 0.65, 5.18$ Hz, 1H), 8.60 (dd, $J = 1.82, 4.86$ Hz, 1H). $[\text{M} + \text{H}]^+ = 471.2$. HRMS $[\text{M} + \text{H}]^+$ calculated for $\text{C}_{25}\text{H}_{29}\text{Cl}_2\text{N}_4\text{O}_1 = 471.1713$, found = 471.1718.

1-(4-(3,5-Dichloro-4-(2-phenylpyridin-3-yl)methoxy)phenyl)pyridin-2-yl)piperazine (82). Prepared using **42** (200 mg, 0.47 mmol, 1 equiv) and (2-phenylpyridin-3-yl)methanol **76** (for synthesis, see Supporting Information) (105 mg, 0.57 mmol, 1.2 equiv), according to the Mitsunobu reaction and BOC deprotection procedure outlined in the synthesis of **51**, to give **82** as an off-white solid (122 mg, 53% yield). ^1H NMR 500 MHz, CDCl_3 , δ 3.03–3.05 (m, 4H), 3.60–3.62 (m, 4H), 5.14 (s, 2H), 6.71 (s, 1H), 6.76 (dd, $J = 1.44, 5.24$ Hz, 1H), 7.41 (dd, $J = 4.76, 7.68$ Hz, 1H), 7.45–7.51 (m, 3H), 7.53 (s, 2H), 7.65–7.67 (m, 2H), 8.22 (dd, $J = 1.65, 7.82$ Hz, 1H), 8.26 (d, $J = 5.21$ Hz, 1H), 8.74 (dd, $J = 1.71, 4.78$ Hz, 1H). $[\text{M} + \text{H}]^+ = 491.2$. HRMS $[\text{M} + \text{H}]^+$ calculated for $\text{C}_{27}\text{H}_{25}\text{Cl}_2\text{N}_4\text{O}_1 = 491.14$, found = 491.1405.

1-(4-(3,5-Dichloro-4-(2-propylpyridin-3-yl)methoxy)phenyl)pyridin-2-yl)piperazine (83). Prepared using **42** (150 mg, 0.35 mmol, 1 equiv) and (2-propylpyridin-3-yl)methanol (**77b**) (for synthesis, see Supporting Information) (63 mg, 0.42 mmol, 1.2 equiv), according to the Mitsunobu reaction and BOC deprotection procedure outlined for the synthesis of **51**, to give **83** as an off-white solid (33 mg, 21% yield). ^1H NMR 500 MHz, CDCl_3 , δ 1.06 (t, $J = 7.53$ Hz, 3H), 1.79–1.87 (m, 2H), 2.96–2.99 (m, 2H), 3.04–3.06 (m, 4H), 3.60–3.63 (m, 4H), 5.14 (s, 2H), 6.74 (s, 1H), 6.78 (dd, $J = 1.40, 5.20$ Hz, 1H), 7.23 (dd, $J = 4.86, 7.55$ Hz, 1H), 7.59 (s, 2H), 7.95 (dd, $J = 1.73, 7.66$ Hz, 1H), 8.28 (dd, $J = 0.70, 5.14$ Hz, 1H), 8.59 (dd, $J = 1.73, 4.87$ Hz, 1H). $[\text{M} + \text{H}]^+ = 457.2$. HRMS $[\text{M} + \text{H}]^+$ calculated for $\text{C}_{24}\text{H}_{27}\text{Cl}_2\text{N}_4\text{O}_1 = 457.1556$, found = 457.1552.

1-(4-(3,5-Dichloro-4-((2-isopentylpyridin-3-yl)methoxy)phenyl)pyridin-2-yl)piperazine (84). Prepared using **42** (150 mg, 0.35 mmol, 1 equiv) and (2-isopentylpyridin-3-yl)methanol (**77c**) (for synthesis, see Supporting Information) (75 mg, 0.42 mmol, 1.2 equiv), according to the Mitsunobu reaction and BOC deprotection procedure outlined for the synthesis of **51**, to give **84** as an off-white solid (109 mg, 65% yield). ^1H NMR 500 MHz, CDCl_3 , δ 1.00 (d, $J = 6.84$ Hz, 6H), 1.65–1.72 (m, 2H), 1.73 (sept, $J = 6.87$ Hz, 1H), 2.97–3.01 (m, 2H), 3.03–3.06 (m, 4H), 3.60–3.63 (m, 4H), 5.14 (s, 2H), 6.74 (s, 1H), 6.78 (dd, $J = 1.39, 5.16$ Hz, 1H), 7.22 (dd, $J = 4.79, 7.74$ Hz, 1H), 7.58 (s, 2H), 7.95 (dd, $J = 1.80, 7.70$ Hz, 1H), 8.28 (dd, $J = 0.61, 5.12$ Hz, 1H), 8.58 (dd, $J = 1.76, 4.92$ Hz, 1H). $[\text{M} + \text{H}]^+ = 485.2$. HRMS $[\text{M} + \text{H}]^+$ calculated for $\text{C}_{26}\text{H}_{31}\text{Cl}_2\text{N}_4\text{O}_1 = 485.1869$, found = 485.1888.

X-ray Crystallography Methods. AfNMT protein–ligand complexes were determined using methods described previously.³⁰ Ternary complexes of AfNMT with myristoyl CoA (MCoA) and ligands of interest were obtained by cocrystallization by incubating protein with 10 mM MCoA plus 10 mM ligand diluted from a 100 mM stock in DMSO prior to crystallization. Diffraction data were measured at the European Synchrotron Radiation Facility (ESRF). Data integration and scaling was carried out using XDS³⁶ and AIMLESS³⁷ or the HKL suite.³⁸ Structures were phased by molecular replacement with MOLREP³⁹ from the CCP4 suite⁴⁰ using the protein coordinates of AfNMT–compound **1** (PDB 4CAX) as a search model. Refinement was carried out using REFMAC5,⁴¹ and manual model alteration was carried out using Coot.⁴² Ligand–coordinate and restraint files were generated using PRODRG,⁴³ and ligands were modeled into unbiased $F_{\text{obs}} - F_{\text{calc}}$ density maps using Coot.

Coordinates of AfNMT–ligand complexes and associated diffraction data have been deposited in the RCSB Protein Data Bank (PDB) with accession codes 5T5U, 5T6C, 5T6E, and 5T6H for compounds **24**, **29**, **48**, and **49**, respectively. Data measurement and refinement statistics are shown in the Supporting Information.

NMT Enzyme Assay. NMT assays^{44,45} were carried out at room temperature (22–23 °C) in 384-well white optiplates (PerkinElmer). Each assay was performed in a 40 μL reaction volume containing 30 mM Tris buffer, pH 7.4, 0.5 mM EDTA, 0.5 mM EGTA, 1.25 mM dithiothreitol (DTT), 0.1% (v/v) Triton X-100, 0.125 μM [³H]-myristoyl-coA (8 Curie (Ci) mmol^{-1}), 0.5 μM biotinylated CAP5.5, 5 nM NMT, and various concentrations of the test compound. The IC_{50} values for HsNMT1 and HsNMT2 were essentially identical against 80 compounds tested, and for logistical reasons, only HsNMT1 was used in later studies.

Test compound (0.4 μL in DMSO) was transferred to all assay plates using a Cartesian Hummingbird (Genomics Solution) before 20 μL of enzyme was added to assay plates. The reaction was initiated with 20 μL of a substrate mix and stopped after 15 min (HsNMT1 or HsNMT2) or 50 min (TbNMT) with 40 μL of a stop solution containing 0.2 M phosphoric acid, pH 4.0, 1.5 M MgCl_2 , and 1 mg mL^{-1} PVT SPA beads (GE Healthcare). All reaction mix additions were carried out using a Thermo Scientific WellMate (Matrix). Plates were sealed and read on a TopCount NXT Microplate Scintillation and Luminescence Counter (PerkinElmer).

ActivityBase from IDBS was used for data processing and analysis. All IC_{50} curve fitting was undertaken using XLFit version 4.2 from IDBS. A four-parameter logistic dose–response curve was used using XLFit 4.2 Model 205. All test compound curves had floating top and bottom, and prefit was used for all four parameters.

Compound Efficacy and Trypanocidal Activity in Cultured *T. brucei* Parasites. Bloodstream *T. b. brucei* s427 was cultured at 37 °C in modified HMI9 medium (56 μM 1-thioglycerol was substituted for 200 μM 2-mercaptoethanol) and quantified using a hemocytometer. For the live/dead assay, cells were analyzed using a two-color cell viability assay (Invitrogen) as described previously.²² Cell culture plates were stamped with 1 μL of an appropriate concentration of test compound in DMSO followed by the addition of 200 μL of trypanosome culture (10^4 cells mL^{-1}) to each well, except for one column, which received media only. MRC-5 cells were cultured in DMEM, seeded at 2000 cells per well, and allowed to adhere overnight. One microliter of test compound (10 point dilutions from 50 μM to 2 nM) was added to each well at the start of the assay. Culture plates of *T. brucei* and MRC-5 cells were incubated at 37 °C in an atmosphere of 5% CO_2 for 69 h, before the addition of 20 μL of resazurin (final concentration, 50 μM). After a further 4 h incubation, fluorescence was measured (excitation 528 nm; emission 590 nm) using a BioTek flx800 plate reader.

■ ASSOCIATED CONTENT

Supporting Information

The Supporting Information is available free of charge on the ACS Publications website at DOI: 10.1021/acs.jmedchem.7b01255.

Experimental details for compounds 3–12 and 17–24; X-ray data collection and refinement statistics; correlation of enzyme activity data for inhibitors against AfNMT and TbNMT; molecular structures of known NMT inhibitors (PDF)

Molecular formulas strings (CSV)

■ AUTHOR INFORMATION

Corresponding Author

*Phone: +44-(0)1382 386 231. E-mail: p.g.wyatt@dundee.ac.uk.

ORCID

David A. Robinson: 0000-0003-1979-5918

Ian H. Gilbert: 0000-0002-5238-1314

Paul G. Wyatt: 0000-0002-0397-245X

Notes

The authors declare no competing financial interest.

■ ACKNOWLEDGMENTS

Funding for this work was provided by the Wellcome Trust (Grant ref. WT077705 and Strategic Award WT083481). We would like to thank Gina McKay for performing HRMS analyses and Daniel James for data management. We thank the European Synchrotron Radiation Facility (ESRF) for synchrotron beamtime and support, and Paul Fyfe for supporting the in-house X-ray facility.

■ ABBREVIATIONS USED

NMT, N-myristoyltransferase; *T. brucei*, *Trypanosoma brucei*; *T. br. brucei*, *T. brucei brucei*; HAT, human African trypanosomiasis or sleeping sickness; CNS, central nervous system; TbNMT, *T. brucei* N-myristoyltransferase; HsNMT, human NMT; LE, ligand efficiency; PSA, polar surface area; AfNMT, *Aspergillus fumigatus* NMT; HBA, hydrogen bond acceptor; HBD, hydrogen bond donor; BBB, blood–brain barrier; MW, molecular weight; cLogP, calculated LogP; cLogD, calculated LogD; SAR, structure–activity relationship; nd, not determined

■ REFERENCES

- (1) Pink, R.; Hudson, A.; Mouries, M. A.; Bendig, M. Opportunities and challenges in antiparasitic drug discovery. *Nat. Rev. Drug Discovery* **2005**, *4*, 727–740.
- (2) WHO. Trypanosomiasis, Human African trypanosomiasis (sleeping sickness). <http://www.who.int/mediacentre/factsheets/fs259/en/> (accessed October 15, 2017).
- (3) Brun, R.; Balmer, O. New developments in human African trypanosomiasis. *Curr. Opin. Infect. Dis.* **2006**, *19*, 415–420.
- (4) Kennedy, P. G. The continuing problem of human African trypanosomiasis (sleeping sickness). *Ann. Neurol.* **2008**, *64*, 116–126.
- (5) Wery, M. Drug used in the treatment of sleeping sickness (human African trypanosomiasis: HAT). *Int. J. Antimicrob. Agents* **1994**, *4*, 227–238.
- (6) Jacobs, R. T.; Nare, B.; Phillips, M. A. State of the art in African trypanosome drug discovery. *Curr. Top. Med. Chem.* **2011**, *11*, 1255–1274.
- (7) Frearson, J. A.; Brand, S.; McElroy, S. P.; Cleghorn, L. A.; Smid, O.; Stojanovski, L.; Price, H. P.; Guthrie, M. L.; Torrie, L. S.; Robinson, D. A.; Hallyburton, I.; Mpamhanga, C. P.; Brannigan, J. A.; Wilkinson, A. J.; Hodgkinson, M.; Hui, R.; Qiu, W.; Raimi, O. G.; van Aalten, D. M.; Brenk, R.; Gilbert, I. H.; Read, K. D.; Fairlamb, A. H.; Ferguson, M. A.; Smith, D. F.; Wyatt, P. G. N-myristoyltransferase inhibitors as new leads to treat sleeping sickness. *Nature* **2010**, *464*, 728–732.
- (8) Hertz-Fowler, C.; Ersfeld, K.; Gull, K. CAP5.5, a life-cycle-regulated, cytoskeleton-associated protein is a member of a novel family of calpain-related proteins in *Trypanosoma brucei*. *Mol. Biochem. Parasitol.* **2001**, *116*, 25–34.
- (9) Price, H. P.; Panethymitaki, C.; Goulding, D.; Smith, D. F. Functional analysis of TbARL1, an N-myristoylated Golgi protein essential for viability in bloodstream trypanosomes. *J. Cell Sci.* **2005**, *118*, 831–841.
- (10) Price, H. P.; Stark, M.; Smith, D. F. *Trypanosoma brucei* ARF1 plays a central role in endocytosis and golgi-lysosome trafficking. *Mol. Biol. Cell* **2007**, *18*, 864–873.
- (11) Price, H. P.; Guthrie, M. L.; Ferguson, M. A.; Smith, D. F. Myristoyl-CoA:protein N-myristoyltransferase depletion in trypanosomes causes avirulence and endocytic defects. *Mol. Biochem. Parasitol.* **2010**, *169*, 55–58.
- (12) Price, H. P.; Menon, M. R.; Panethymitaki, C.; Goulding, D.; McKean, P. G.; Smith, D. F. Myristoyl-CoA:protein N-myristoyltransferase, an essential enzyme and potential drug target in kinetoplastid parasites. *J. Biol. Chem.* **2003**, *278*, 7206–7214.
- (13) Farazi, T. A.; Waksman, G.; Gordon, J. I. The biology and enzymology of protein N-myristoylation. *J. Biol. Chem.* **2001**, *276*, 39501–39504.

- (14) Wright, M. H.; Clough, B.; Rackham, M. D.; Rangachari, K.; Brannigan, J. A.; Grainger, M.; Moss, D. K.; Bottrill, A. R.; Heal, W. P.; Broncel, M.; Serwa, R. A.; Brady, D.; Mann, D. J.; Leatherbarrow, R. J.; Tewari, R.; Wilkinson, A. J.; Holder, A. A.; Tate, E. W. Validation of N-myristoyltransferase as an antimalarial drug target using an integrated chemical biology approach. *Nat. Chem.* **2014**, *6*, 112–121.
- (15) Wright, M. H.; Paape, D.; Storck, E. M.; Serwa, R. A.; Smith, D. F.; Tate, E. W. Global analysis of protein N-myristoylation and exploration of N-myristoyltransferase as a drug target in the neglected human pathogen *Leishmania donovani*. *Chem. Biol.* **2015**, *22*, 342–354.
- (16) Herrera, L. J.; Brand, S.; Santos, A.; Nohara, L. L.; Harrison, J.; Norcross, N. R.; Thompson, S.; Smith, V.; Lema, C.; Varela-Ramirez, A.; Gilbert, I. H.; Almeida, I. C.; Maldonado, R. A. Validation of N-myristoyltransferase as Potential Chemotherapeutic Target in Mammal-Dwelling Stages of *Trypanosoma cruzi*. *PLoS Neglected Trop. Dis.* **2016**, *10*, e0004540.
- (17) Roberts, A. J.; Fairlamb, A. H. The N-myristoylome of *Trypanosoma cruzi*. *Sci. Rep.* **2016**, *6*, 31078.
- (18) Ritzefeld, M.; Wright, M. H.; Tate, E. W. New developments in probing and targeting protein acylation in malaria, leishmaniasis and African sleeping sickness. *Parasitology* **2017**, 1–18.
- (19) Rampoldi, F.; Bonrouhi, M.; Boehm, M. E.; Lehmann, W. D.; Popovic, Z. V.; Kaden, S.; Federico, G.; Brunk, F.; Grone, H. J.; Porubsky, S. Immunosuppression and aberrant T cell development in the absence of N-myristoylation. *J. Immunol.* **2015**, *195*, 4228–4243.
- (20) Das, U.; Kumar, S.; Dimmock, J. R.; Sharma, R. K. Inhibition of protein N-myristoylation: a therapeutic protocol in developing anticancer agents. *Curr. Cancer Drug Targets* **2012**, *12*, 667–692.
- (21) Thionon, E.; Morales-Sanfrutos, J.; Mann, D. J.; Tate, E. W. N-Myristoyltransferase Inhibition Induces ER-Stress, Cell Cycle Arrest, and Apoptosis in Cancer Cells. *ACS Chem. Biol.* **2016**, *11*, 2165–2176.
- (22) Brand, S.; Cleghorn, L. A.; McElroy, S. P.; Robinson, D. A.; Smith, V. C.; Hallyburton, I.; Harrison, J. R.; Norcross, N. R.; Spinks, D.; Bayliss, T.; Norval, S.; Stojanovski, L.; Torrie, L. S.; Frearson, J. A.; Brenk, R.; Fairlamb, A. H.; Ferguson, M. A.; Read, K. D.; Wyatt, P. G.; Gilbert, I. H. Discovery of a novel class of orally active trypanocidal N-myristoyltransferase inhibitors. *J. Med. Chem.* **2012**, *55*, 140–152.
- (23) Brand, S. W. P.; Thompson, S.; Smith, V.; Bayliss, T.; Harrison, J.; Norcross, N.; Cleghorn, L.; Gilbert, I.; Brenk, R. N-Myristoyl transferase inhibitors. Patent WO2010026365, 2010.
- (24) Brand, S.; Norcross, N. R.; Thompson, S.; Harrison, J. R.; Smith, V. C.; Robinson, D. A.; Torrie, L. S.; McElroy, S. P.; Hallyburton, I.; Norval, S.; Scullion, P.; Stojanovski, L.; Simeons, F. R. C.; van Aalten, D.; Frearson, J. A.; Brenk, R.; Fairlamb, A. H.; Ferguson, M. A. J.; Wyatt, P. G.; Gilbert, I. H.; Read, K. D. Lead optimization of a pyrazole sulfonamide series of *Trypanosoma brucei* N-myristoyltransferase inhibitors: Identification and evaluation of CNS penetrant compounds as potential treatments for stage 2 human african trypanosomiasis. *J. Med. Chem.* **2014**, *57*, 9855–9869.
- (25) Hopkins, A. L.; Groom, C. R.; Alex, A. Ligand efficiency: a useful metric for lead selection. *Drug Discovery Today* **2004**, *9*, 430–431.
- (26) Ebiike, H.; Masubuchi, M.; Liu, P.; Kawasaki, K.; Morikami, K.; Sogabe, S.; Hayase, M.; Fujii, T.; Sakata, K.; Shindoh, H.; Shiratori, Y.; Aoki, Y.; Ohtsuka, T.; Shimma, N. Design and synthesis of novel benzofurans as a new class of antifungal agents targeting fungal N-myristoyltransferase. Part 2. *Bioorg. Med. Chem. Lett.* **2002**, *12*, 607–610.
- (27) Masubuchi, M.; Kawasaki, K.; Ebiike, H.; Ikeda, Y.; Tsujii, S.; Sogabe, S.; Fujii, T.; Sakata, K.; Shiratori, Y.; Aoki, Y.; Ohtsuka, T.; Shimma, N. Design and synthesis of novel benzofurans as a new class of antifungal agents targeting fungal N-myristoyltransferase. Part 1. *Bioorg. Med. Chem. Lett.* **2001**, *11*, 1833–1837.
- (28) Sogabe, S.; Masubuchi, M.; Sakata, K.; Fukami, T. A.; Morikami, K.; Shiratori, Y.; Ebiike, H.; Kawasaki, K.; Aoki, Y.; Shimma, N.; D'Arcy, A.; Winkler, F. K.; Banner, D. W.; Ohtsuka, T. Crystal structures of *Candida albicans* N-myristoyltransferase with two distinct inhibitors. *Chem. Biol.* **2002**, *9*, 1119–1128.
- (29) Armour, D. R.; Bell, A. S.; Kemp, M. I.; Edwards, M. P.; Wood, A. Discovery of a novel series of non-peptidic fungal N-myristoyltransferase inhibitors. 221st ACS National Meeting, San Diego, CA, United States, April 1–5, 2001; p MEDI-349.
- (30) Fang, W.; Robinson, D. A.; Raimi, O. G.; Blair, D. E.; Harrison, J. R.; Lockhart, D. E.; Torrie, L. S.; Ruda, G. F.; Wyatt, P. G.; Gilbert, I. H.; van Aalten, D. M. N-myristoyltransferase is a cell wall target in *Aspergillus fumigatus*. *ACS Chem. Biol.* **2015**, *10*, 1425–1434.
- (31) Patani, G. A.; LaVoie, E. J. Bioisosterism: A rational approach in drug design. *Chem. Rev.* **1996**, *96*, 3147–3176.
- (32) Clark, D. E. In silico prediction of blood-brain barrier permeation. *Drug Discovery Today* **2003**, *8*, 927–933.
- (33) Hitchcock, S. A.; Pennington, L. D. Structure-brain exposure relationships. *J. Med. Chem.* **2006**, *49*, 7559–7583.
- (34) Yu, Z.; Brannigan, J. A.; Moss, D. K.; Brzozowski, A. M.; Wilkinson, A. J.; Holder, A. A.; Tate, E. W.; Leatherbarrow, R. J. Design and synthesis of inhibitors of *Plasmodium falciparum* N-myristoyltransferase, a promising target for antimalarial drug discovery. *J. Med. Chem.* **2012**, *55*, 8879–8890.
- (35) Shultz, M. D. Setting expectations in molecular optimizations: Strengths and limitations of commonly used composite parameters. *Bioorg. Med. Chem. Lett.* **2013**, *23*, 5980–5991.
- (36) Kabsch, W. Xds. *Acta Crystallogr., Sect. D: Biol. Crystallogr.* **2010**, *66* (Pt 2), 125–32.
- (37) Evans, P. R.; Murshudov, G. N. How good are my data and what is the resolution? *Acta Crystallogr., Sect. D: Biol. Crystallogr.* **2013**, *69*, 1204–1214.
- (38) Otwinowski, Z.; Minor, W.; Carter, C. W.; Sweet, R. M. Processing of X-ray diffraction data collected in oscillation mode. *Methods Enzymol.* **1997**, *276*, 307–326.
- (39) Vagin, A.; Teplyakov, A. Molecular replacement with MOLREP. *Acta Crystallogr., Sect. D: Biol. Crystallogr.* **2010**, *66*, 22–25.
- (40) Winn, M. D.; Ballard, C. C.; Cowtan, K. D.; Dodson, E. J.; Emsley, P.; Evans, P. R.; Keegan, R. M.; Krissinel, E. B.; Leslie, A. G.; McCoy, A.; McNicholas, S. J.; Murshudov, G. N.; Pannu, N. S.; Potterton, E. A.; Powell, H. R.; Read, R. J.; Vagin, A.; Wilson, K. S. Overview of the CCP4 suite and current developments. *Acta Crystallogr., Sect. D: Biol. Crystallogr.* **2011**, *67*, 235–242.
- (41) Murshudov, G. N.; Skubak, P.; Lebedev, A. A.; Pannu, N. S.; Steiner, R. A.; Nicholls, R. A.; Winn, M. D.; Long, F.; Vagin, A. A. REFMAC5 for the refinement of macromolecular crystal structures. *Acta Crystallogr., Sect. D: Biol. Crystallogr.* **2011**, *67*, 355–67.
- (42) Emsley, P.; Cowtan, K. Coot: model-building tools for molecular graphics. *Acta Crystallogr., Sect. D: Biol. Crystallogr.* **2004**, *60*, 2126–2132.
- (43) Schuttelkopf, A. W.; van Aalten, D. M. PRODRG: a tool for high-throughput crystallography of protein-ligand complexes. *Acta Crystallogr., Sect. D: Biol. Crystallogr.* **2004**, *60*, 1355–1363.
- (44) Bowyer, P. W.; Gunaratne, R. S.; Grainger, M.; Withers-Martinez, C.; Wickramasinghe, S. R.; Tate, E. W.; Leatherbarrow, R. J.; Brown, K. A.; Holder, A. A.; Smith, D. F. Molecules incorporating a benzothiazole core scaffold inhibit the N-myristoyltransferase of *Plasmodium falciparum*. *Biochem. J.* **2007**, *408*, 173–180.
- (45) Panethymitaki, C.; Bowyer, P. W.; Price, H. P.; Leatherbarrow, R. J.; Brown, K. A.; Smith, D. F. Characterization and selective inhibition of myristoyl-CoA:protein N-myristoyltransferase from *Trypanosoma brucei* and *Leishmania major*. *Biochem. J.* **2006**, *396*, 277–285.